PEDRO VELLOSO GOMES BATISTA

MODELAGEM DA EROSÃO HÍDRICA E MÉTODOS DE INTERPOLAÇÃO DE BATIMETRIA FLUVIAL NA BACIA DO ALTO RIO GRANDE (MG)

LAVRAS – MG

2016

PEDRO VELLOSO GOMES BATISTA

MODELAGEM DA EROSÃO HÍDRICA E MÉTODOS DE INTERPOLAÇÃO DE BATIMETRIA FLUVIAL NA BACIA DO ALTO RIO GRANDE (MG)

Dissertação apresentada à Universidade Federal de Lavras, como parte das exigências do Programa de Pós Graduação em Ciência do Solo, área de concentração em Recursos Ambientais e Uso da Terra, para a obtenção do título de Mestre.

Orientador

Dr. Marx Leandro Naves Silva

LAVRAS – MG

2016

Ficha catalográfica elaborada pelo Sistema de Geração de Ficha Catalográfica da Biblioteca Universitária da UFLA, com dados informados pelo próprio autor.

Batista, Pedro Velloso Gomes.
Modelagem da erosão hídrica e métodos de interpolação de batimetria fluvial na bacia do Alto Rio Grande (MG) / Pedro Velloso Gomes Batista. – Lavras : UFLA, 2016.
107 p. : il.

Dissertação (mestrado acadêmico)–Universidade Federal de Lavras, 2016.
Orientador(a): Marx Leandro Naves Silva.
Bibliografia.

1. Erosão. 2. Rusle. 3. Sedd. 4. Krigagem Por Regressão. 5. Batimetria. I. Universidade Federal de Lavras. II. Título.

PEDRO VELLOSO GOMES BATISTA

MODELAGEM DA EROSÃO HÍDRICA E MÉTODOS DE INTERPOLAÇÃO DE BATIMETRIA FLUVIAL NA BACIA DO ALTO RIO GRANDE (MG)

Dissertação apresentada à Universidade Federal de Lavras, como parte das exigências do Programa de Pós Graduação em Ciência do Solo, área de concentração em Recursos Ambientais e Uso da Terra, para a obtenção do título de Mestre.

APROVADA em 12 de fevereiro de 2016.

Dr. Nilton Curi	UFLA
Dr. Marcelo Silva de Oliveira	UFLA
Dr. Velibor Spalevic	University of Montenegro
Dr. John Quinton	Lancaster University

Dr. Marx Leandro Naves Silva

Orientador

LAVRAS – MG

2016

A meus pais, Antônio e Wanessa,

minha irmã, Cecília,

e meus avós, Laércio e Rosa Maria.

DEDICO

AGRADECIMENTOS

À Universidade Federal de Lavras (UFLA) e ao Departamento de Ciência do Solo (DCS), pela formação acadêmica e oportunidade de pesquisa.

À Fundação de Amparo à Pesquisa do Estado de Minas Gerais (FAPEMIG), à Coordenação de Aperfeiçoamento de Pessoal de Nível Superior (CAPES) e ao Conselho Nacional de Desenvolvimento Científico e Tecnológico (CNPq) pela concessão de bolsas de estudo.

Ao professor Marx Leandro Naves Silva, pela orientação, apoio e confiança transmitida desde a iniciação científica. Ao professor Marcelo Silva de Oliveira, pelo ensino da geoestatística. Aos professores do DCS, pelo conhecimento transmitido e, em especial, à professora Michele Menezes e ao professor Nilton Curi, pelo auxílio neste estudo. Aos funcionários do DCS, pelo contínuo apoio.

Aos colegas de pós-graduação do DCS, pela amizade e companheirismo. Em especial aos meus grandes amigos Diego Tassinari, Bárbara Silva, Pedro Lima, Diego Faustolo e Lucas Pontes. Ao colega e amigo Fabio Arnaldo, pela enorme contribuição neste trabalho e por todos os estudos que desenvolvemos juntos, que influenciaram grandemente minha formação científica.

À minha família, meu grande tesouro, pela educação que me ofereceu. À minha mãe, que me ensinou o inglês que, finalmente, veio tanto a calhar; ao meu pai e ao meu avô, pelo gosto pelas plantas e pelas coisas que são da terra, e ao meu tio e padrinho, Luiz Eduardo, pela primeira coleção de rochas.

À República Villa Velha, onde fiz minha casa quando vim para Lavras, em 2008.

“And I followed you, Big River, when you called.”

J. R. Cash

RESUMO

A erosão hídrica afeta negativamente a estrutura e a fertilidade do solo, além limitar a disponibilidade de água para plantas. Ademais, os impactos *ex-situ* da erosão contribuem para a sedimentação e eutrofização de cursos d'água. Em bacias hidrográficas, modelos preditores da erosão são usados para avaliar tais impactos de maneira distribuída. Levantamentos batimétricos de rios e reservatórios oferecem importantes informações em relação aos impactos *ex-situ* da erosão, uma vez que mudanças geomorfológicas devido à sedimentação podem ser analisadas a partir de modelos de terreno derivados de pontos batimétricos. Porém, como levantamentos batimétricos extensivos despendem grandes recursos, as medições de profundidade de corpos d'água são geralmente realizadas em seções batimétricas, o que pode levar a formação de uma malha amostral esparsa. O objetivo deste estudo foi estimar as perdas de solo, entrega de sedimentos e produção total sedimentos na bacia hidrográfica do Alto Rio Grande, usando a Revised Universal Soil Loss Equation (RUSLE) e o modelo Sediment Delivery Distributed (SEDD) e, assim, estimar a entrega de sedimentos aos principais reservatórios de usinas hidrelétricas da bacia. Ademais, objetivou-se avaliar métodos híbridos de krigagem para interpolação de pontos batimétricos de um trecho inundado do Rio Grande. A distância ortogonal à linha de centro do rio foi usada como uma variável auxiliar para krigagem por regressão (KR) e co-krigagem (CK). Os resultados dos métodos híbridos foram comparados aos da krigagem ordinária, inverso da distância ponderada e Topogrid, através de uma validação externa. As predições da RUSLE estimaram que as perdas de solo médias na bacia do Alto Rio Grande são de 22,35 t ha^{-1} ano^{-1}, e que solos descobertos, eucalipto e agricultura constituem os usos do solo mais propensos à erosão na bacia. A produção específica de sedimentos média na bacia foi de 1,93 t ha^{-1} ano^{-1}. De acordo com a calibração dos modelos, tal predição apresentou um erro de 0,02 t ha^{-1} ano^{-1}, ou 1,25%. As predições dos modelos estimaram que 1,45 milhões de t ano^{-1} de sedimentos são entregues ao reservatório de Camargos/Itutinga, enquanto o reservatório do Funil recebe um aporte de 1,59 milhões de t ano^{-1} de sedimentos. Apesar da calibração dos modelos ter apresentado um baixo erro em relação aos dados sedimentométricos observados, a baixa disponibilidade de dados de campo não permitiu uma validação mais robusta dos métodos empregados. Ainda assim, os resultados indicam que a combinação dos modelos RUSLE/SEDD pode ser útil para a análise do transporte de sedimentos em bacias hidrográficas no Brasil. A validação externa dos métodos híbridos de krigagem indicou que a abordagem da KR adotada rendeu os menores erros quadráticos médios dentre os interpoladores analisados. Ademais, no mapa resultante da KR, o talvegue foi preservado nas grandes lacunas não amostradas entre as seções batimétricas, enquanto os demais métodos subestimaram a

profundidade do talvegue em tais espaços. Assim, conclui-se que o método de KR empregado neste estudo propiciou uma abordagem simples para diminuir o erro da predição espacial a partir de dados esparsos de batimetria.

Palavras-chave: Erosão. RUSLE. SEDD. Krigagem por regressão. Batimetria.

ABSTRACT

Water erosion negatively affects soil fertility, soil structure, and water availability to plants. Moreover, the off-site erosion impacts contribute to the sedimentation and eutrophication of water courses. At watershed scale, erosion models are used to evaluate such impacts in a distributed manner. Bathymetric surveys from rivers and reservoirs can supply important information regarding off-site erosion effects, since geomorphologic changes due to sedimentation can be assessed from bathymetry-derived terrain models. However, since extensive bathymetric surveys may prove to be costly and time consuming, water depth measurements are usually made through cross-sectional surveys, which may lead to a sparse sampling pattern. The aim of this study was to estimate the soil losses and sediment yield in the Upper Grande River Basin, using the Revised Universal Soil Loss Equation (RUSLE) and the Sediment Delivery Distributed model (SEDD); and also, to quantify the sediment delivery to the main hydroelectric power plant reservoirs in the basin. Moreover, it aimed to evaluate hybrid kriging methods for interpolating bathymetry point data from a flooded segment of the Grande River. The orthogonal distance to river centerline was used as an auxiliary variable for regression kriging (RK) and co-kriging (CK). The results from the hybrid kriging methods were compared to the ones from ordinary kriging, inverse distance weighting and topogrid, through an external validation. RUSLE predictions estimated that the average soil losses in the Upper Grande River Basin were of 22.35 t ha^{-1} yr^{-1}, and that bare soils, eucalypt and agriculture suffered the highest erosion rates among the identified land use classes. The average specific sediment yield (SSY) in the basin was of 1.93 t ha^{-1} yr^{-1}. According to the SEDD model calibration, the SSY predictions showed an error of 0.02 t ha^{-1} yr^{-1}, or 1.25%. The model predictions estimated that 1.45 million t yr^{-1} of sediments are delivered to the Camargos/Itutinga power plant reservoir, whereas the Funil power plant reservoir receives a sediment input of 1.59 million t yr^{-1}. Although model calibration yielded small errors in relation to the observed data, the lack of field measurements has impaired a more thorough validation of the employed models. Nevertheless, the results indicate that the RUSLE/SEDD approach may be useful for analyzing sediment transport in Brazilian watersheds, where limited input data is available. The external validation of the hybrid kriging methods indicated that the employed RK approach yielded the lowest RMSE among the analyzed interpolators. Moreover, the RK predictions were able to represent the river thalweg between the widely spaced cross-sections, whereas the other methods under-predicted the thalweg in such gaps. Therefore, we concluded that the employed RK method provided a simple approach for enhancing the quality of the spatial prediction from sparse bathymetry data.

Key-words: Erosion. RUSLE. SEDD. Regression kriging. Bathymetry.

SUMÁRIO

PRIMEIRA PARTE

INTRODUÇÃO

Modelos científicos podem ser definidos como uma descrição interpretativa de um fenômeno (BAILER-JONES, 2009). Tal descrição deve, portanto, compreender os processos que compõem, ou produzem, o dado fenômeno, através de um componente teórico e da observação do objeto de estudo. Porém, diversos fenômenos na natureza são o produto de uma interação tão complexa de processos que sua realização pode parecer aleatória, ou pelo menos, não explicável através de uma solução matemática ou determinística (OLIVER; WEBSTER, 2014).

Dessa forma, a criação de modelos nas ciências naturais é uma tarefa intricada, especialmente quando se deseja fazer predições sobre a realização de um fenômeno através de um modelo. Isto é, quando o modelo é um meio para prever o comportamento de um fenômeno em outro ponto no espaço ou no tempo (BEVEN, 2012). A natureza preditiva dos modelos científicos é importante em diversos campos das ciências naturais, uma vez que sua aplicação permite que se antevejam impactos ambientais decorrentes de ações antrópicas (WAINWRIGTH; MULLIGAN, 2013).

Os modelos preditores da erosão, sobre os quais se concentra este estudo, surgiram devido a uma crescente preocupação pública com as consequências negativas das perdas de solo em terras agrícolas, muito evidenciadas após o “Dust Bowl”, nos EUA, na década de 1930 (RENSCHLER; HARBOR, 2002). Assim, a Universal Soil Loss Equation (USLE) foi desenvolvida a partir da necessidade de um modelo abrangente para a predição

quantitativa da erosão hídrica em solos cultivados, o que auxiliaria no planejamento conservacionista do uso da terra (WISCHMEIER; SMITH, 1978).

A USLE é um modelo empírico em que fatores numéricos são usados para descrever a influência da precipitação pluvial, do solo, da topografia e da cobertura e manejo do solo em relação à erosão hídrica. A Revised Universal Soil Loss Equation (RUSLE), uma versão revisada da USLE proposta por Renard et al. (1997), manteve os fatores estabelecidos na equação original, incorporando, porém, melhorias em relação à representação espacial e temporal de tais fatores. Devido à estrutura simples de ambas USLE e RUSLE, tais equações foram amplamente utilizadas no estudo da erosão, especialmente em situações em que há uma limitação para obtenção dos diversos dados de entrada exigidos por modelos mais sofisticados (MERRITT; LETCHER; JAKEMAN, 2003).

A partir do avanço das tecnologias de geoprocessamento e do desenvolvimento dos Sistemas de Informações Geográficas (SIG), as equações da USLE e RUSLE foram adaptadas para análise da erosão em largas escalas. A aplicação de tais modelos através de SIG tornou-se uma ferramenta importante para avaliação da erosão em bacias hidrográficas, uma vez que tal abordagem permite que as taxas de perdas de solo sejam modeladas de forma contínua no espaço geográfico (AKSOY; KAVVAS, 2005).

Uma limitação dos modelos USLE e RULSE é que os resultados de suas equações oferecem apenas estimativas de erosão bruta, isto é, a deposição ao longo das vertentes e a entrega de sedimentos aos cursos d'água não são representadas pelos modelos, o que dificulta a análise dos impactos *ex-situ* da erosão. Para lidar com tal limitação, Ferro e Minacapilli (1995) e Ferro e Porto (2000) desenvolveram um método para o cálculo, geograficamente distribuído, da taxa de entrega de sedimentos em bacias hidrográficas, ou seja, do percentual

de sedimentos erodidos que são carreados até a rede de drenagem. Este método consiste no Sediment Delivery Distributed model (SEDD), um modelo semi-empírico em que a taxa de entrega de sedimentos em um dado ponto é baseada no tempo percorrido pelo escoamento superficial neste ponto até o curso d'água mais próximo. No SEDD, as estimativas de erosão bruta da RUSLE são combinadas com as taxas de entrega de sedimentos para se modelar espacialmente a produção de sedimentos em bacias hidrogáficas. Uma vez que os sedimentos entregues aos cursos d'água são responsáveis pelo assoreamento de rios, lagos e reservatórios, a identificação dos locais com maior produção específica de sedimentos é essencial para o planejamento conservacionista (SILVA; CURI, 2001; FERNANDEZ et al., 2003).

O assoreamento de reservatórios é um dos impactos *ex-situ* mais relevantes da erosão, já que a deposição acelerada de sedimentos em represas de usinas hidrelétricas reduz sua capacidade de armazenamento de água, o que limita a vida útil das usinas (VERSTRAETEN et al., 2003). As taxas de assoreamento em reservatórios, porém, podem oferecer dados importantes quanto à produção de sedimentos nas bacias localizadas à montante das represas. De acordo com de Vente et al. (2013), levantamentos batimétricos em reservatórios, temporalmente espaçados, fornecem as estimativas mais acuradas sobre a produção de sedimentos em bacia hidrográficas, já que a variabilidade temporal de eventos extremos é melhor representada do que a partir de medições sedimentométricas pontuais.

O cálculo preciso da taxa de assoreamento de reservatórios, baseado na diferença entre superfícies num espaço de tempo, porém, depende da geração de modelos contínuos da topografia submersa, que são produzidos através da interpolação de pontos batimétricos discretos. Além disso, modelos digitais de elevação da topografia submersa de rios e reservatórios são usados para análise

de mudanças geomorfológicas e para simulações hidrológicas (MERWADE, 2009; GLENN et al., 2015).

A interpolação de dados batimétricos apresenta, porém, alguns desafios. Uma vez que a batimetria é tradicionalmente realizada em seções transversais, a malha amostral pode exibir grandes lacunas de áreas não levantadas, localizadas entre as seções batimétricas (LEGLEITER, 2013). Uma possível abordagem geoestatística para esta questão pode partir do uso de métodos híbridos de krigagem, em que, além da auto-correlação espacial da variável resposta, a correlação com variáveis auxiliares é usada para melhorar a predição espacial (HENGL, 2009). Em tais métodos, informações espacialmente exaustivas de mapas auxiliares são usadas para modelar o componente determinístico da variabilidade espacial da variável resposta, cujos valores são conhecidos apenas nas observações pontuais amostradas (HENGL; HEUVELINK; ROSSITER, 2007).

O Rio Grande é um dos principais afluentes do Rio Paraná, que é o segundo maior rio em comprimento na América do Sul e a principal fonte de energia hidrelétrica no Brasil. A bacia hidrográfica do Alto Rio Grande é particularmente relevante quanto geração de energia hidrelétrica em Minas Gerais, pois fornece água para duas importantes usinas, Camargos/Itutinga e Funil, que juntas possuem uma capacidade de geração de 280 MW. Estudos recentes indicam uma elevada propensão à erosão hídrica na Bacia do Alto Rio Grande, devido à susceptibilidade dos solos e à ausência de práticas conservacionistas na agricultura (BESKOW et al., 2009; GOMIDE; SILVA; SOARES, 2011; SOARES, 2015). Nesse caso, além dos impactos *in-situ* da erosão, como a perda de matéria orgânica e nutrientes do solo, o comprometimento dos recursos hídricos devido à sedimentação e ao assoreamento de cursos d’água cosnsiste em um sério problema ambiental.

Dessa forma, este trabalho teve como objetivo: i) modelar as perdas de solo, taxas de entrega de sedimentos e produção de sedimentos na bacia do Alto Rio Grande, através dos modelos RUSLE e SEDD, em ambiente SIG; ii) analisar métodos híbridos de krigagem como alternativa para a otimização da interpolação de dados batimétricos escassos, baseados em levantamentos realizados em um trecho inundado do Rio Grande, no reservatório do Funil.

REFERÊNCIAS BIBLIOGRÁFICAS

AKSOY, H.; KAVVAS, M. L. A review of hillslope and watershed scale erosion and sediment transport models. **Catena**, v. 64, p. 247–271, 2005.

BAILER-JONES, D. M. **Scientific Models in Philosophy of Science.** Pittsburgh: University of Pittsburgh Press, 2009. 235p.

BESKOW, S.; MELLO, C. R.; NORTON, L. D.; CURI, N.; VIOLA, M. R.; AVANZI, J. C. Soil erosion prediction in the Grande River Basin, Brazil using distributed modeling. **Catena**, v. 79, n. 1, p. 49–59, 2009.

BEVEN, K. **Rainfall-runoff modeling**: the primer. West Sussex: John Wiley & Sons, 2012. 457p.

DE VENTE, J.; POESEN, J.; VERSTRAETEN, G.; GOVERS, G.; VANMAERCKE, M.; VAN ROMPAEY, A.; ARABKHEDRI, M.; BOIX-FAYOS, C. Predicting soil erosion and sediment yield at regional scales: Where do we stand? **Earth-Science Reviews**, v. 127, p. 16–29, 2013.

FERNANDEZ, C.; WU, J. Q.; MCCOOL, D. K.; STOCKLE, C. O. Estimating water erosion and sediment yield with GIs , RUSLE , and SEDD. **Journal of Soil and Water Conservation**, v. 58, p. 128–136, 2003.

FERRO, V.; MINACAPILLI, M. Sediment delivery processes at basin scale. **Hydrological Sciences Journal**, v. 40, n. 6, p. 703–717, 1995.

FERRO, V.; PORTO, P. Sediment Delivery Distributed (SEDD) Model. **Journal Of Hydrologic Engineering**, v. 5, n. 4, p. 411–422, 2000.

GLENN, J; TONINA, D.; MOREHEAD, M. D.; FIEDLER, F.; BENJAKAR, R. Effect of transect location, transect spacing and interpolation methods on river bathymetry accuracy. **Earth Surface Processes and Landforms**, p. n/a–n/a, 2015.

GOMIDE, P. H. O.; SILVA, M. L. N.; SOARES, C. R. F. S. Atributos físicos, químcos e biológicos do solo em ambientes de voçorocas no município de Lavras - MG. **Revista Brasileira de Ciência do Solo**, v. 35, p. 567–577, 2011.

HENGL, T.; HEUVELINK, G. B. M.; ROSSITER, D. G. About regression-kriging: From equations to case studies. **Computers & Geosciences**, v. 33, n. 10, p. 1301–1315, 2007.

HENGL, T. **A Practical Guide to Geostatiscal Mapping**. Luxembourg: Office for Official Publications of the European Communities, 2009. 143 p.

LEGLEITER, C. J. Mapping river depth from publicly available aerial images. **River Research and Applications**, v. 29, p. 760–780, 2013.

MERRITT, W. S.; LETCHER, R. A.; JAKEMAN, A. J. A review of erosion and sediment transport models. **Environmental Modelling & Software**, v. 18, n. 8-9, p. 761–799, 2003.

MERWADE, V. Effect of spatial trends on interpolation of river bathymetry. **Journal of Hydrology**, v. 371, n. 1-4, p. 169–181, 2009.

OLIVER, M. A.; WEBSTER, R. A tutorial guide to geostatistics: Computing and modelling variograms and kriging. **Catena**, v. 113, p. 56–69, 2014.

RENARD, K. G.; FOSTER, G. R.; WEESIES, G. A.; MCCOOL, D. K.; YODER, D. C. **Predicting soil erosion by water: a guide to conservation planning with the Revised Universal Soil Loss Equation**. Washington: U.S. Department of Agriculture, 1997. 384p.

RENSCHLER, C. S.; HARBOR, J. Soil erosion assessment tools from point to regional scales—the role of geomorphologists in land management research and implementation. **Geomorphology**, v. 47, n. 2-4, p. 189–209, 2002.

SILVA, M. L. N.; CURI, N. Uso e conservação do solo e da água e a crise energética: reflexões e exemplos em Minas Gerais. **Sociedade Brasileira de Ciência do Solo** – Boletim informativo, v.26, n.4, p. 10-13, 2001.

SOARES, W. S. **Taxa de assoreamento no reservatório da Usina Hidrelétrica do Funil - MG.** 2015. 45p. MS Thesis – Universidade Federal de Lavras, Lavras, 2015.

VERSTRAETEN, G.; POESEN, J.; DE VENT, J.; KONINCKX, X. Sediment yield variability in Spain: a quantitative and semiqualitative analysis using reservoir sedimentation rates. **Geomorphology**, v. 50, n. 4, p. 327–348, 2003.

WAINWRIGHT, J.; MULLIGAN, M. **Environmental Modeling**: finding simplicity in complexity. West Sussex: John Wiley & Sons, 2013. 494p.

WISCHMEIER, W. H.; SMITH, D. D. **Predicting rainfall erosion losses**: **a guide to conservation planning**. Washington: USDA, 1978. 58 p.

REVISÃO DE LITERATURA

Erosão hídrica e modelos de predição de perdas de solo em bacias hidrográficas

A produção de sedimentos em uma bacia hidrográfica é predominantemente decorrente do desprendimento e arraste de partículas do solo por meio da erosão hídrica, que pode ser definida como o processo de desgaste da superfície terrestre pela ação da água, que destaca ou remove o solo ou seu material geológico de origem de um ponto da superfície e o deposita em outro (SSSA, 2008). Com esta definição, é possível separar o processo erosivo em três etapas distintas: o desprendimento, o transporte e a deposição de partículas do solo ou seu material de origem.

A erosão hídrica degrada a estrutura do solo e reduz os teores de matéria orgânica e de nutrientes, limitando a camada cultivável do solo (MORGAN, 2005; DOTTERWEICH, 2013). Além disso, a infiltração de água é prejudicada pela erosão, o que contribui para redução da umidade do solo e da disponibilidade de água para culturas (PIMENTEL, 2006). Dessa forma, os impactos *in-situ* da erosão afetam a produção de biomassa, alimentos e fibras, reduzindo a produtividade de lavouras e aumentando a necessidade de aplicação de fertilizantes (RENSCHLER; HARBOR, 2002; POESEN, 2011).

Apesar dos efeitos diretos *in-situ* da erosão em áreas agrícolas serem relevantes, os impactos *ex-situ* deste fenômeno são motivo de grande preocupação ambiental, especialmente em relação à sedimentação e eutrofização de cursos d'água (HU et al., 2009; OUYANG et al., 2010; WU et al., 2012). O material erodido, quando não encontra algum impedimento físico, é carregado ao longo da rede de drenagem da bacia para corpos de água superficiais e

subterrâneos (SILVA; CURI, 2001). À medida que os sedimentos são depositados nos cursos d'água, a capacidade de armazenamento de rios e reservatórios diminui, o que aumenta o risco de inundações (MORGAN, 2005). O assoreamento de reservatórios é um dos principais efeitos negativos da erosão *ex-situ*, uma vez que a redução da capacidade de armazenamento afeta a vida útil de usinas hidrelétricas (VERSTRAETEN et al., 2003)

Devido à dificuldade de realizarem-se medições diretas da erosão no campo, o desenvolvimento de modelos preditores da erosão hídrica tem recebido grande atenção por parte de cientistas do solo. Os primeiros modelos empíricos de erosão foram desenvolvidos nos EUA ainda na década de 1940, culminando com a formação da Universal Soil Loss Equation (USLE) (WISCHMEIER & SMITH, 1978) e sua versão revisada (RUSLE) (RENARD et al., 1997). Ambas USLE e RULSE são amplamente utilizadas, uma vez que sua estrutura simples é desejável em situações em que há uma pequena disponibilidade de dados (RENSCHLER; HARBOR, 2002; MERRITT; LETCHER; JAKEMAN, 2003). Apesar da existência de modelos mais sofisticados, a RUSLE ainda é comumente usada para análise da erosão em largas escalas, através de Sistemas de Informações Geográficas (SIG) (XU; XU; MENG, 2013; PANAGOS et al., 2015; XIAOYING et al., 2015). A aplicação de tais modelos através de SIG tornou-se uma ferramenta importante para avaliação da erosão em bacias hidrográficas, uma vez que tal abordagem permite que as perdas de solo sejam modeladas de forma contínua no espaço geográfico (AKSOY; KAVVAS, 2005).

Uma limitação dos modelos USLE e RULSE é que os resultados de suas equações oferecem apenas estimativas de erosão bruta, isto é, a deposição ao longo das vertentes e a entrega de sedimentos aos cursos d'água não são representadas pelos modelos, o que dificulta a análise dos impactos *ex-situ* da erosão. Devido ao fato de apenas uma parte dos sedimentos desprendidos nas

vertentes de bacias hidrográficas alcançar os cursos d'água e o ponto de eflúvio da bacia, uma taxa de entrega de sedimentos (TES) é usada para expressar o percentual de erosão bruta que eventualmente contribui para a produção de sedimentos, definida como a quantidade de sedimentos que é descarregada pelo canal principal (WALLING, 1994). Os padrões e taxas da distribuição de sedimentos em bacias hidrográficas dependem de vários fatores, como área de drenagem, localização das fontes de sedimentos, topografia, uso do solo e textura do solo (WALLING, 1994; VANMAERCKE et al., 2011). Dessa forma, uma análise espacialmente distribuída da TES é essencial para a avalição dos impactos *ex-situ* da erosão e para o planejamento conservacionista do solo (FERNANDEZ et al., 2003).

O modelo Sediment Delivery Distributed (SEDD) (FERRO; MINACAPILLI, 1995; FERRO; PORTO, 2000) oferece uma estimativa espacializada, semi-empírica, da TES em bacias hidrográficas. Os cálculos são baseados no tempo percorrido pelo escoamento superficial, em um dado local, ao longo do caminho hidráulico até o curso d'água mais próximo. De acordo com Ferro e Porto (2000), todos os sedimentos entregues à rede de drenagem são eventualmente descarregados no ponto de eflúvio da bacia, considerando-se um longo período de análise. Dessa forma, o processo de entrega de sedimentos poderia ser simplifado ao se desconsiderar sua deposição nos canais. No SEDD, as estimativas de erosão bruta da RUSLE são combinadas com as taxas de entrega de sedimentos para se modelar espacialmente a produção específica sedimentos em bacias hidrogáficas, o que possiblita a identificação das principais fontes de sedimentos na área de estudo. Tal metodologia foi aplicada desde em microbacias na Espanha (TAGUAS et al., 2011) e na Itália (STEFANO; FERRO, 2007), bem como em grandes bacias hidrográficas na Turquia (TANYAŞ; KOLAT; SÜZEN, 2015) e China (YANG et al, 2012).

Assoreamento de reservatórios: relevância, dinâmica e monitoramento

Atualmente, 63,63% da capacidade de geração de energia elétrica no Brasil é proveniente de Usinas Hidrelétricas (UHE) (ANELL, 2014), cujo princípio de funcionamento consiste basicamente no aproveitamento da energia do fluxo da água que se move a partir de um ponto de elevação superior no relevo em direção a um ponto de elevação inferior e, por isso, é considerada uma fonte de energia renovável. Apesar da instalação de uma UHE exigir um alto investimento financeiro inicial, argumenta-se que a longa vida útil e o baixo custo de operação e manutenção deste tipo de empreendimento o torna economicamente competitivo (KUMAR et al., 2011). Porém, o processo de assoreamento em reservatórios reduz sua capacidade de armazenamento e pode, quando muito agravado, comprometer antecipadamente o funcionamento de uma UHE.

Entende-se, portanto, que o assoreamento de reservatórios pode limitar a vida útil de um empreendimento hidrelétrico e este processo pode ser agravado pelo manejo das bacias hidrográficas à montante (LOCHER; SCALON, 2012). Dessa forma, é imperativo o monitoramento do assoreamento e da sedimentação em reservatórios e seus afluentes, bem como os mecanismos de produção destes sedimentos em suas respectivas bacias de contribuição.

O assoreamento de reservatórios segue padrões, que devem ser estudados e quantificados para predizerem-se os tipos de danos que serão causados ao aproveitamento, bem como a faixa de tempo em que ocorrerão tais danos e quais estratégias poderão ser empregadas para minimizá-los (MORRIS; FAN 1998).

De acordo com Carvalho et al. (2000), o reservatório causa a redução das velocidades das correntes dos cursos d'água – que tem suas seções transversais aumentadas ao adentrá-lo, criando condições favoráveis à deposição de sedimentos. Enquanto as partículas mais pesadas são depositadas primeiramente, as partículas mais finas adentram o reservatório. A barragem, porém, apresenta um impedimento à passagem dos sedimentos à jusante.

Devido a estes padrões desuniformes, ocorrem no reservatório três tipos principais de deposição: delta, depósito de margem e depósito de leito. O delta é formado principalmente por partículas grossas, as primeiras a se depositarem, enquanto os demais são caracteristicamente formados por partículas finas que adentram o reservatório por correntes de turbidez (CARVALHO et al., 2000).. Além destas formas de deposição, a erosão por deslizamento de massas nas margens do reservatório, a ocorrência de enchentes extremas ou o rebaixamento da represa podem formar outros tipos de deposição, com materiais finos e grossos (MORRIS; FAN, 1998; CARVALHO et al., 2000).

Quando o aproveitamento se encontra em fase de operação, os estudos sedimentológicos são concentrados entorno do monitoramento das estações sedimentométricas instaladas à montante do reservatório e levantamentos batimétricos da área represada (CARVALHO et al., 2000).

A batimetria consiste na medição e mapeamento de profundidades para representar topograficamente o fundo do oceano ou outros corpos d'água (KEARNS; BREMAN, 2010). No Brasil, o monitoramento do assoreamento em reservatórios deve ser feito por meio de levantamentos batimétricos, obrigatoriamente realizados por ecobatímetros, de acordo com as orientações da Agência Nacional de Águas (ANA). Este tipo de levantamento possibilita a medição da elevação do fundo do corpo d'água em vários pontos, georreferenciados, ao longo de seções espalhadas pelo reservatório.

Por meio de técnicas de predição espacial, é possível interpolar informações de elevação contidas em vetores (pontos, linhas ou polígonos) para gerar Modelos Digitais de Elevação (MDE), que representam valores de elevação de forma contínua no espaço.

Interpolação de dados batimétricos de rios e reservatórios

A criação de MDEs precisos para representação contínua da topografia submersa de rios e reservatórios é desejável para fornecer uma base adequada para estimativas de assoreamento, cálculos de capacidade de armazenamento e simulações hidrológicas (MERWADE, 2009). Tais modelos são gerados a partir da interpolação de pontos obtidos em levantamentos batimétricos, tradicionalmente realizados em seções transversais ao fluxo do rio (MERWADE et al., 2008; SCHÄPPI et al., 2010).

Apesar do desenvolvimento recente de técnicas apuradas de geoestatística para a interpolação de dados batimétricos (MERWADE et al., 2005; MERWADE et al., 2006, MERWADE et al., 2008), poucos trabalhos no Brasil dedicaram-se ao tema (ALCÂNTRA et al., 2010; LOPES et al., 2013). Além disso, observa-se, por experiência de campo e pela literatura científica especializada, que a interpolação prévia ao cálculo do volume de reservatórios é geralmente realizada por meio de métodos mecânicos (ALBERTIN et al., 2010; MIRANDA et al., 2013), em detrimento de interpoladores geoestatísticos.

A malha amostral obtida pelo levantamento batimétrico tradicional restringe o desempenho de interpoladores, já que áreas consideráveis compreendidas entre seções não são amostradas. Ademais, MERWADE et al. (2006) destacam que a anisotropia inerente à morfologia fluvial (a variabilidade da elevação é maior transversalmente à direção do fluxo do que ao longo do

fluxo; a direção do leito do rio é inconsistente devido sua sinuosidade) dificulta a interpolação geoestatística de dados batimétricos.

Variáveis explanatórias ou mesmo mapas auxiliares podem aperfeiçoar o desempenho de formas mais simples de krigagem, ao adicionar informações exaustivamente espacializadas às observações pontuais amostradas para variável resposta (HENGL et al., 2007). De acordo com HENGL et al. (2004), a krigagem por regressão (KR) – em que uma ou mais variáveis auxiliares são usadas para definir o componente determinístico da predição espacial a partir de um modelo linear (Hengl, 2009), produz, em muitos casos, resultados melhores e mais detalhados do que técnicas comuns de geoestatística.

Formas de krigagem com uso de variáveis explanatórias têm sido aplicadas a diversas áreas das geociências, especialmente na modelagem da topografia (HENGL et al., 2008), atributos do solo (QI-YONG et al.; 2014) ou até mesmo na batimetria marinha (JEROSCH, 2013).

REFERÊNCIAS BIBLIOGRÁFICAS

ALBERTIN, L. L.; MATOS, A. J. S.; MAUAD, F. F. Cálculo do Volume e Análise da Deposição de Sedimentos do Reservatório de Três Irmãos. **Revista Brasileira de Recursos Hídricos**, v. 15, p.57-67, 2010.

ALCÂNTRA, E.; NOVO, E.; STECH, J.; ASSIREU, A.; NASCIMENTO, R.; LORENZZETTI, J.; SOUZA, A. Integrating historical topographic maps and SRTM data to derive the bathymetry of a tropical reservoir. **Journal of Hydrology**, v.389, p.311-316, 2010.

ANEEL. Banco de informações de geração. Disponível em: <http://www.aneel.gov.br/aplicacoes/capacidadebrasil/capacidadebrasil.cfm>. Acesso em: 19 de jun. 2014.

AKSOY, H.; KAVVAS, M. L. A review of hillslope and watershed scale erosion and sediment transport models. **Catena**, v. 64, p. 247–271, 2005.

CARVALHO, N. O; FILIZOLA JR., SANTOS, P. M. C; LIMA, J. E. F. W. **Guia de avaliação de assoreamento de reservatórios**. Brasília : ANEEL, 132p. 2000.

DOTTERWEICH, M. The history of human-induced soil erosion: Geomorphic legacies, early descriptions and research, and the development of soil conservation—A global synopsis. **Geomorphology**, v. 201, p. 1–34, 2013.

FERNANDEZ, C.; WU, J. Q.; MCCOOL, D. K.; STOCKLE, C. O. Estimating water erosion and sediment yield with GIs , RUSLE , and SEDD. **Journal of Soil and Water Conservation**, v. 58, p. 128–136, 2003.

FERRO, V.; MINACAPILLI, M. Sediment delivery processes at basin scale. **Hydrological Sciences Journal**, v. 40, n. 6, p. 703–717, 1995.

FERRO, V.; PORTO, P. Sediment Delivery Distributed (SEDD) Model. **Journal Of Hydrologic Engineering**, v. 5, n. 4, p. 411–422, 2000.

HENGL, T.; HEUVELINK, G. B. M.; STEIN, A. A generic framework for spatial prediction of soil variables based on regression-kriging. **Geoderna**, v.120, p. 75-93, 2004.

HENGL, T.; HEUVELINK, G. B. M.; ROSSITER, D. G. About regression-kriging: From equations to case studies. **Computers & Geosciences**, v. 33, p.1301-1315, 2007.

HENGL, T.; BAJAT, B.; BLAGOJEVIC, D.; REUTER, H. I.; Geostatistical modeling of topography using auxiliary maps. **Computers & Geosciences**, v.34, p. 1886-1899, 2008.

HU, B.; YANG, Z.; WANG, H.; SUN, X.; BI, N.; LI, G. Sedimentation in the Three Gorges Dam and the future trend of Changjiang (Yangtze River) sediment flux to the sea. **Hidrology and Earth System Sciences**, v. 13, p. 2253–2264, 2009.

JEROSCH, K. Geostatistical mapping and spatial variability of surficial sediment types on the Beaufort Shelf based on grain size data. **Journal of Marine Systems**, v. 127, p.5-13, 2013.

KEARNS, A.; BREMAN, J. **Bathymetry - The art and science of seafloor modeling for modern applications**. In: BREMAN, J. (Ed.) Ocean Globe, Redlands, ESRI Press, 2010, p.1-36.

KUMAR, A., SCHEI, T.; AHENKORAH, A.; CACERES, R.; DEVERNAY, J.M.; FREITAS, M.; HALL, D.; KILLINGTVEIT, A.; LIU, Z. Hidropower. In: EDENHOFER, O; PICHS-MADRUGA, R.; SOKONA, Y.; SEYBOTH, K.; MATSCHOSS, P.; KADNER, S.; ZWICKEL, T.; EICKEMEIER, P.; HANSEN, G.; SCHLÖMER, S.; VON STECHOWIPCC, C. (Orgs.). **Special Report on Renewable Energy Sources and Climate Change Mitigation**. Cambridge, United Kingdom : 2001, p. 437-496.

LOCHER, H.; SCANLON, A. Sustainable Hydropower – Issues and Approaches. BOROUJENI, S.H. (Ed.). In: **Hydropower – Practice and Aplication**, InTech, 2012. Disponível em: <http://www.intechopen.com/books/hydropower-practice-and-application/sustainable-hydropower-issues- and-approaches>.

LOPES, H. L.; NETO, A. R.; CIRILO, J. A. Modelagem batimétrica no reservatório de Sobradinho: I – geração e avaliação de superfícies batimétricas utilizando interpoladores espaciais. **Revista Brasileira de Cartografia**, v. 65, p.907-922, 2013.

MERRITT, W. S.; LETCHER, R. A.; JAKEMAN, A. J. A review of erosion and sediment transport models. **Environmental Modelling & Software**, v. 18, n. 8-9, p. 761–799, 2003.

MERWADE, V.; MAIDMENT, D. R.; HODGES, B. R. Geospatial representation of river channels. **Journal of Hydrologic Engeneering**,, v.10, p.243-251, 2005.

MERWADE, V.; MAIDMENT, D. R.; GOFF, J. A. Anisotropic considerations while interpolating river bathymetry. **Journal of Hidrology**, v.331, p.731-741, 2006.

MERWADE, V.; COOK, A.; COONROD, J. GIS techniques for creating river terrain models for hydrodynamic modeling and flood inundation mapping. **Environmental Modelling & Software**, v.23, p.1300-1311, 2008.

MERWADE, V. Effect of spatial trends on interpolation of river bathymetry. **Journal of Hydrology**, v. 371, n. 1-4, p. 169–181, jun. 2009.

MORGAN, R. P. C. **Soil Erosion and Conservation**. 3rd ed. Oxford: Blackwell Publishing, 2005. 299 p.

MORRIS, G.L.; FAN, J. **Reservoir sedimentation handbook**. McGrawll-Hill Book Co., 1998. 848 p.

OUYANG, W.; HAO, F.; SKIDMORE, A. K.; TOXOPEUS, A. G. Soil erosion and sediment yield and their relationships with vegetation cover in upper stream of the Yellow River. **The Science of the total environment**, v. 409, n. 2, p. 396–403, 2010.

PANAGOS, P.; BORRELLI, P.; MEUSBURGER, K.; ALEWELL, C.; LUGATO, E.; MONTANARELLA, L. Estimating the soil erosion cover-management factor at the European scale. **Land Use Policy**, v. 48, p. 38–50, 2015.

PIMENTEL, D. Soil Erosion: A Food and Environmental Threat. **Environment, Development and Sustainability**, v. 8, n. 1, p. 119–137, 2006.

POESEN, J. Challenges in gully erosion research. **Landform Analysis**, v. 17, p. 5–9, 2011.

QI-YONG, Y.; ZHONG-CHENG, J.; WEN-JUN, L; HUI, L. Prediction of soil organic matter in peak-cluster depression region using kriging and terrain indices. **Soil and Tillage Research**, v. 144, p. 126-132, 2014.

RENARD, K. G.; FOSTER, G. R.; WEESIES, G. A.; MCCOOL, D. K.; YODER, D. C. **Predicting soil erosion by water: a guide to conservation planning with the Revised Universal Soil Loss Equation**. Washington: U.S. Department of Agriculture, 1997. 384p.

RENSCHLER, C. S.; HARBOR, J. Soil erosion assessment tools from point to regional scales—the role of geomorphologists in land management research and implementation. **Geomorphology**, v. 47, n. 2-4, p. 189–209, 2002.

TAGUAS, E. V.; MORAL, C.; AYUSO, J. L.; PEREZ, R.; GOMEZ, J. A. Modeling the spatial distribution of water erosion within a Spanish olive orchard microcatchment using the SEDD model. **Geomorphology**, v. 133, n. 1-2, p. 47–56, 2011.

TANYAŞ, H.; KOLAT, Ç.; SÜZEN, M. L. A new approach to estimate cover-management factor of RUSLE and validation of RUSLE model in the watershed of Kartalkaya Dam. **Journal of Hydrology**, v. 528, p. 584–598, 2015.

SCHÄPPI, B.; PERONA, P.; SCHNEIDER, P.; BURLANDO, P. Integrating river cross section measurements with digital terrain models for improved flow modelling applications. **Computers & Geosciences**, v.36, p.707-716, 2010.

SILVA, M. L. N.; CURI, N. Uso e conservação do solo e da água e a crise energética: reflexões e exemplos em Minas Gerais. **Sociedade Brasileira de Ciência do Solo** – Boletim informativo, v.26, n.4, p. 10-13, 2001.

SOARES, W. S. **Taxa de assoreamento no reservatório da Usina Hidrelétrica do Funil - MG.** 2015. 45p. MS Thesis – Universidade Federal de Lavras, Lavras, 2015.

STEFANO, C. DI; FERRO, V. Evaluation of the SEDD model for predicting sediment yield at the Sicilian experimental SPA2 basin. **Earth Surface Processes and Landforms,** v. 32, p. 1094–1109, 2007.

WALLING, D. E. Measuring sediment yield from river basins. In: LAL, R. **Soil erosion research methods**. Washington: Soil and Water Conservation Society; 1994. p.39-82.

SOIL SCIENCE SOCIETY OF AMERICA. **Glossary of soil science terms**. Madison, 2008. 88 p.

VANMAERCKE, M.; POESEN, J.; VERSTRAETEN, G.; DE VENTE, J.; OCAKOGLU, F. Sediment yield in Europe: Spatial patterns and scale dependency. **Geomorphology**, v. 130, n. 3-4, p. 142–161, 2011.

VERSTRAETEN, G.; POESEN, J.; DE VENT, J.; KONINCKX, X. Sediment yield variability in Spain: a quantitative and semiqualitative analysis using reservoir sedimentation rates. **Geomorphology**, v. 50, n. 4, p. 327–348, 2003.

WISCHMEIER, W. H.; SMITH, D. D. **Predicting rainfall erosion losses**: **a guide to conservation planning**. Washington: USDA, 1978. 58 p.

WU, C.-H.; CHEN, C. N.; TSAI, C. H.; TSAI, C. T. Estimating sediment deposition volume in a reservoir using the physiographic soil erosion-deposition model. **International Journal of Sediment Research**, v. 27, n. 3, p. 362–377, 2012.

XIAOYING, L.; QI, S.; HUANG, Y.; CHEN, Y.; DU, P. Predictive modeling in sediment transportation across multiple spatial scales in the Jialing River Basin of China. **International Journal of Sediment Research**, v. 30, n. 3, 2015.

XU, L.; XU, X.; MENG, X. Risk assessment of soil erosion in different rainfall scenarios by RUSLE model coupled with Information Diffusion Model: A case study of Bohai Rim, China. **Catena**, v. 100, p. 74–82, 2013.

YANG, M.; LI, X.; HU, Y.; HE, X. Assessing effects of landscape pattern on sediment yield using sediment delivery distributed model and a landscape indicator. **Ecological Indicators**, v. 22, p. 38–52, 2012.

SEGUNDA PARTE – ARTIGOS

ARTIGO 1 - MODELING SOIL LOSSES AND SEDIMENT YIELD IN THE UPPER GRANDE RIVER BASIN, BRAZIL

ABSTRACT

Water erosion negatively affects soil fertility, soil structure, and water availability to plants. Moreover, the effects of off-site erosion contribute to the sedimentation and eutrophication of water courses. The Grande River is one of the main tributaries of the Paraná River, and an important source of hydroelectric power in Brazil. The Upper Grande River Basin covers an area of 15,705 km², mostly occupied by native pastures dedicated to dairy cattle raising. Shallow and little permeable Cambisols are the predominant soil class in the basin, which, combined with the intensive and highly concentrated summer rainfall, characterize an erosion-prone scenario. The aim of this study was to model the soil losses and the sediment yield in the Upper Grande River Basin. It also sought to quantify the sediment delivery to the two main hydroelectric power plant reservoirs in the basin: Camargos/Itutinga and Funil. Geographical Information Systems (GIS) were used to apply the Revised Universal Soil Loss Equation (RUSLE) and the Sediment Delivery Distributed model (SEDD) in the study area. The models were calibrated using sediment transport data obtained from a river gauging station located in a subwatershed. RUSLE predictions estimated that the average soil losses in the Upper Grande River Basin were of 22.35 t ha^{-1} yr^{-1}, and that bare soils, eucalypt and agriculture suffered the highest erosion rates among the identified land use classes. The results also indicated that eucalypt forests are associated with very erodible soils and steep hillslopes, and, therefore, should receive special attention regarding soil conservation planning. The average specific sediment yield in the basin was of 1.93 t ha^{-1} yr^{-1}. According to the model calibration, the specific sediment yield predictions showed an error of 0.02 t ha^{-1} yr^{-1}, or 1.25%. Agriculture and eucalypt forests, which compose approximately 10% of the study area, contribute to more than 40% of the sediment yield in the basin. The model predictions estimated that 1.45 million t yr^{-1} of sediments are delivered to the Camargos/Itutinga power plant reservoir, whereas the Funil power plant reservoir receives a sediment input of 1.59 million t yr^{-1}. Therefore, sedimentation rates should be higher in the latter case. Although model calibration yielded small errors in relation to the observed sediment measurements, the lack of available data has impaired a more thorough validation of the employed models. Nevertheless, the results indicate

that the RUSLE/SEDD approach may be useful for analyzing sediment transport in Brazilian watersheds, where limited input data is available.

Key-words: Erosion. Sediment delivery. RUSLE. SEDD. GIS.

RESUMO

A erosão hídrica afeta negativamente a estrutura e a fertilidade do solo, além limitar a disponibilidade de água para plantas. Ademais, os efeitos *ex-situ* da erosão contribuem para a sedimentação e eutrofização de cursos d'água. O Rio Grande, um dos principais afluentes do Rio Paraná, é reconhecidamente importante em relação à geração de energia hidrelétrica no Brasil. A bacia do Alto Rio Grande cobre uma área de 15.705 km², predominantemente ocupada por pastagens nativas voltadas para a criação de gado leiteiro. Cambissolos, marcadamente rasos e pouco permeáveis, constituem a principal classe de solo na bacia e, combinados com a precipitação pluvial intensa e cocentrada durante o verão, caracterizam um ambiente propício à erosão. O objetivo deste estudo foi modelar as perdas de solo e produção de sedimentos na bacia do Alto Rio Grande e dessa, forma, quantificar a entrega de sedimentos até os principais reservatórios de usinas hidrelétricas na bacia. Para tal, Sistemas de Informações Geográficas (SIG) foram usados para aplicar a Revised Universal Soil Loss Equation (RUSLE) e o Sediment Delivery Destributed Model (SEDD) na área de estudo. Os modelos foram calibrados a partir de medições sedimentométricas de uma estação localizada em um sub-bacia. As predições da RUSLE estimaram que as perdas de solo médias na bacia do Alto Rio Grande são de 22,35 t ha^{-1} ano^{-1}, e que solos descobertos, eucalipto e agricultura constituem os usos do solo mais propensos à erosão na bacia. Os resultados também indicaram que florestas de eucalipto, na área de estudo, estão associadas a solos altamente erodíveis e a vertentes declivosas e, portanto, devem receber atenção especial em relação ao planejamento conservacionista do uso do solo. A produção específica de sedimentos média na bacia foi de 1,93 t ha^{-1} ano^{-1}. De acordo com a calibração dos modelos, tal predição apresentou um erro de 0,02 t ha^{-1} ano^{-1}, ou 1,25%. A agricultura e o cultivo do eucalipto, que juntas compõem 10% da área de estudo, contribuem para mais de 40% da produção total de sedimentos na bacia do Alto Rio Grande. As predições dos modelos estimaram que 1,45 milhões de t ano^{-1} de sedimentos são entregues ao reservatório de Camargos/Itutinga, enquanto o reservatório do Funil recebe um aporte de 1,59 milhões de t ano^{-1} de sedimentos. Apesar da calibração dos modelos ter apresentado um baixo erro em relação aos dados sedimentométricos observados, a baixa disponibilidade de dados de campo não permitiu uma validação mais robusta dos métodos empregados. Ainda assim, os resultados indicam que a combinação dos modelos RUSLE/SEDD pode ser útil para a análise do transporte de sedimentos em bacias hidrográficas no Brasil.

Palavras-chave: Erosão. Entrega de sedimentos. RUSLE. SEDD. SIG.

INTRODUCTION

Water erosion degrades soil structure, lowers soil organic matter and nutrient contents, thus reducing cultivable soil depth and depleting soil fertility (MORGAN, 2005; DOTTERWEICH, 2013). Erosion also decreases water absorption, which lowers soil moisture and water availability to plants (PIMENTEL, 2006) On-site soil erosion affects not only biomass, food and fiber production, but also diminishes farm income since it lowers cropland yields and increases the necessity of fertilizer applications (RENSCHLER; HARBOR, 2002; POESEN, 2011).

Although the direct effects of on-site erosion on agricultural lands are relevant, off-site erosion impacts have drawn great concern, especially regarding the sedimentation and eutrophication of water courses (HU et al., 2009; OUYANG et al., 2010; WU et al., 2012). As upland eroded sediments reach the stream network, river capacity reduces, and flood risk increases (MORGAN, 2005). Reservoir sedimentation is also one of the most relevant off-site erosion consequences, since it lowers water storage capacity and shortens the lifespan of hydroelectric power plants (VERSTRAETEN et al., 2003).

Since direct erosion measurements are costly and time consuming, the development of soil erosion prediction models has received much attention from soil scientists. Early empirical erosion models were developed in the USA during the 1940's and culminated with the Universal Soil Loss Equation (USLE) (WISCHMEIER & SMITH, 1978) and its revised version (RUSLE) (RENARD et al., 1997). USLE and RUSLE have been widely used, as their simple approach is useful where limited input data is available (RENSCHLER; HARBOR, 2002; MERRITT; LETCHER; JAKEMAN, 2003). Although more

sophisticated, deductive, and less empirical models are now accessible, RUSLE is still commonly employed, particularly at larger scales, through Geographic Information Systems (GIS) (XU; XU; MENG, 2013; PANAGOS et al., 2015a; XIAOYING et al., 2015). The combination of erosion prediction models with GIS has proved to be a powerful tool for evaluating soil losses at catchment scale, enabling the assessment of erosion rates in a distributive manner (AKSOY; KAVVAS, 2005).

However, RUSLE outputs only estimations of gross erosion, providing little information on sediment delivery to water courses. Since only a fraction of upland eroded sediments reaches the catchment outlet, a sediment delivery ratio (SDR) is used to express the rate of gross erosion that eventually contributes to a river basin sediment yield (WALLING, 1994). Sediment delivery and sediment yield from river basins offer relevant data regarding off-site erosion. Sediment transport rates and patterns depend on many factors, such as catchment area, location of sediment sources, topographic characteristics, land use and soil texture (WALLING, 1994; VANMAERCKE et al., 2011). Therefore, a spatially distributed analysis of sediment delivery at watershed scale is critical in order to properly measure the impacts of off-site erosion and to plan conservation strategies (FERNANDEZ et al. 2003).

The Sediment Delivery Distributed (SEDD) model (FERRO; MINACAPILLI, 1995; FERRO; PORTO, 2000) provides an empirical and spatially distributed calculation of SDR. It is based on particle travel time from a given location to the nearest stream channel, following the hydraulic path of the overland flow. Ferro and Porto (2000) have suggested that during a long-period analysis, all sediments that reach the stream network are eventually discharged through the basin outlet. Therefore, the sediment delivery process could be simplified by neglecting channel deposition. The combination of RUSLE annual

gross erosion predictions with SEDD by GIS processing provides an estimation of river basin sediment yield and a spatial identification of sediment sources. Such methodology has been applied in microcatchments in Spain (TAGUAS et al., 2011) and Italy (STEFANO; FERRO, 2007), as well as in large river basins in Turkey (TANYAŞ; KOLAT; SÜZEN, 2015) and China (YANG et al., 2012). To the author's knowledge, however, the SEDD model has not yet been tested under tropical conditions, such as in Brazilian watersheds.

The State of Minas Gerais, Brazil, has a strategic importance concerning water resources in Brazil and South America. The state holds the springs of Grande, Parnaíba and São Francisco rivers. The first two are the main tributaries of the Paraná River, the second longest river in South America and the main source of hydroelectric power in the country. The Upper Grande River Basin is particularly relevant regarding hydroelectric power generation, since it supplies water to two important power plants: Camargos/Itutinga and Funil, which combined have a 280 MW generation capacity.

The Upper Grande River Basin received some of earliest settlements during the colonization of the State of Minas Gerais, thus suffering environmental impacts from mining and agriculture since the late 17th century. Reports of accelerated erosion and gully formation on the northern portion of the basin can be tracked to the 19th century (BURTON, 1889). More recently, studies indicate a high erosion propensity within the Upper Grande River basin due to the erodibility of the soils and the absence of agricultural conservation practices (BESKOW et al., 2009; GOMIDE; SILVA; SOARES, 2011). However, the lack of river gauging stations in the region hampers direct measurements of sediment concentration in the water, which highlights the importance of erosion and sediment delivery prediction models. Given the large

size of Brazilian river basins and the coarse available data, erosion models must be able to provide useful information from a restricted database.

Hence, the aim of this study was to apply the RUSLE and SEDD models, using GIS, to predict the soil losses, sediment delivery rates, and sediment yield within the Upper Grande River basin, making it possible to identify the main sediment sources in the basin; and also, to estimate the sediment budget that annually reaches the main reservoirs of hydroelectric power plants in the basin.

MATERIAL AND METHODS

Study area

The Upper Grande River Basin covers an area of 15,705 km². It stretches from the Grande River spring, in the Mantiqueira mountain range, to the Mortes River mouth, at the Funil hydroelectric power plant reservoir. On the left bank of the Grande River, about 2 km upstream from the Mortes River mouth, the Capivari River flows into the reservoir. Therefore, three main subwatersheds can be defined: the Mortes River sub-basin, to the north; the Grande River sub-basin, in the central and southern regions; and the Capivari River sub-basin, to the west. The reservoir of the Camargos/Itutinga power plant is also located at the Grande River, approximately 30 km upstream from the Funil reservoir (Figure 1). The first has a 798 hm³ water storage capacity, whilst the latter stores 260 hm³.

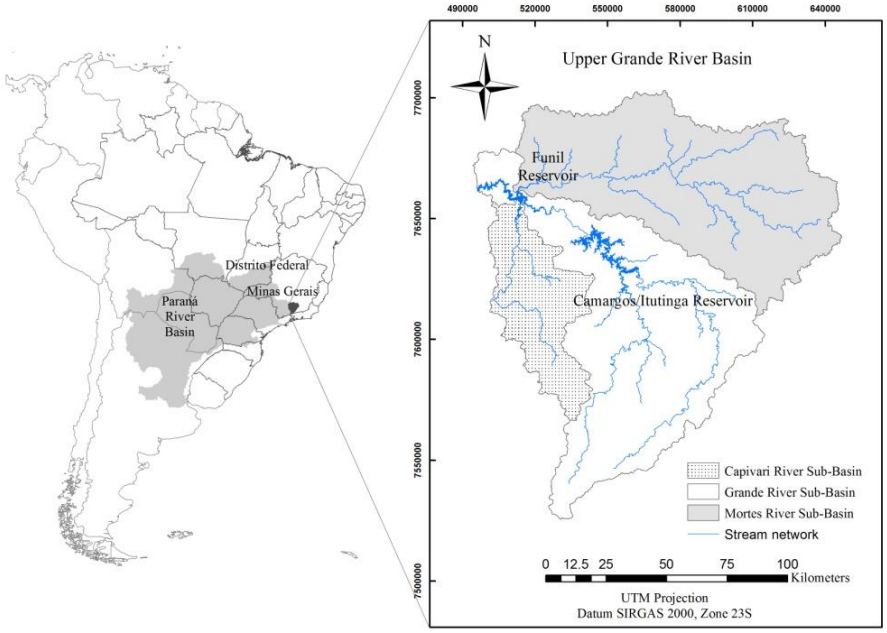

Figure1 Location of the Upper Grande River Basin

According to the Köppen climatic classification, the prevailing climate type in the study area is Cwb – Humid subtropical with dry winter and temperate summer, with an average annual precipitation of 1567 mm (HIJMANS et al., 2005; ALVARES et al., 2013). Granit-gneiss from the crystalline basement and pelitic rocks are the prevailing geological components, followed by quartzite rocks from the ridge formations (CPRM, 2003). Haplic Cambisols and Red Yellow Latosols are the predominant soil classes, spreading through 44% and 31% of the study area, respectively (FEAM, 2010). Haplic Cambisols are shallow, not much permeable and often graveled, usually associated to hilly, mountainous slopes; Red Yellow Latosols are severely weathered, deep, very permeable soils, usually found in the flatter, gentle slopes along the landscape (MENEZES et al., 2009). Rangeland is the primary land use, frequently degraded by overgrazing and water erosion.

RUSLE modeling

RUSLE estimates average annual soil losses by a direct equation in which five empirical factors are used to describe the processes affecting erosion (RENARD et al., 1997):

$$A = R * K * LS * C * P \quad (1)$$

where: A is soil loss per unit area (t ha^{-1} yr^{-1}); R is the rainfall and runoff erosivity factor (MJ mm ha^{-1} h^{-1} yr^{-1}); K is soil erodibility factor (t ha h ha^{-1} MJ^{-1} mm^{-1}); LS is the topographic factor, representing slope length and steepness (dimensionless); C is cover management factor (dimensionless), and P is support practice factor (dimensionless).

For spatial modeling purposes, ArcGIS 10.1 (ESRI, 2011) was used to compose grid layers of each RULSE factor, enabling the application of map algebra tools to the georeferenced grid cell values. The methodologies for composing these layers, as well as the necessary input data (Figure 2), are described as follows.

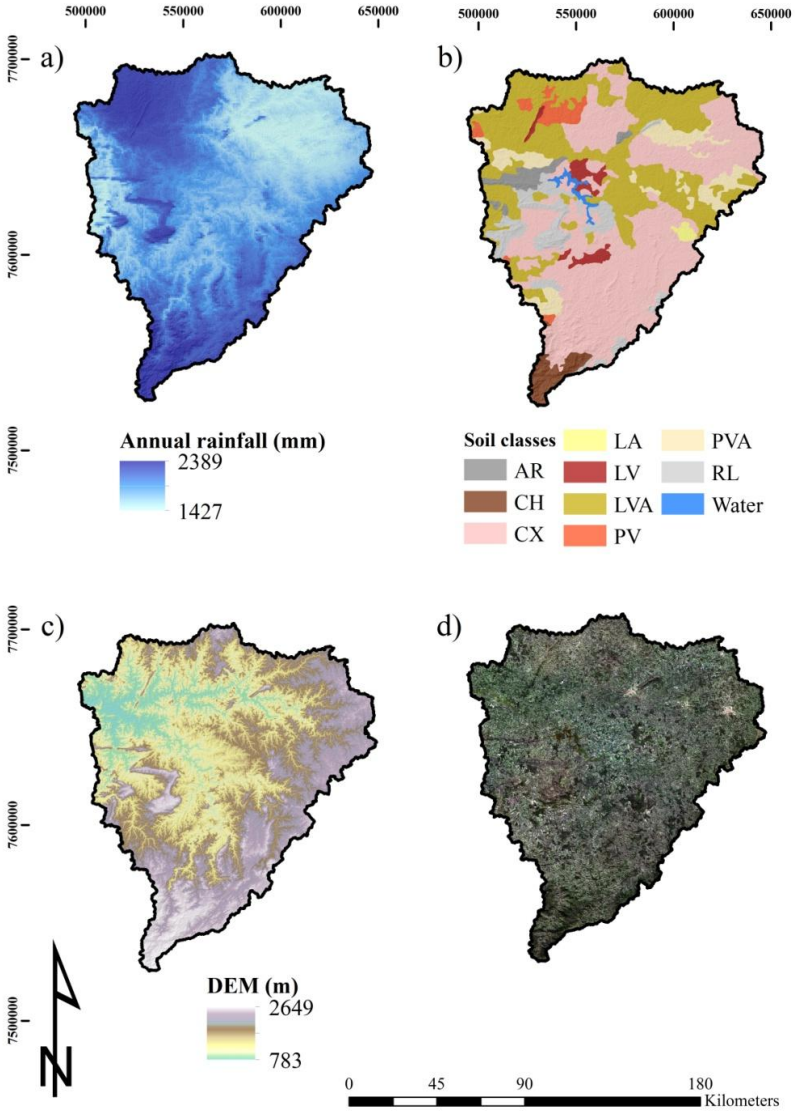

Figure 2 GIS input data for RUSLE modeling in the Upper Grande River Basin: annual rainfall grid (a); soil map (b); Digital Elevation Model (c); Landsat imagery (d). Legend: AR: Rock outcrop; CH: Humic Cambisol; CX: Haplic Cambisol; LA: Yellow Latosol; LV: Red Latosol; LVA: Red Yellow Latosol; PV: Red Argisol; PVA: Red Yellow Argisol; RL: Litholic Neosol

Rainfall-runoff erosivity factor (R)

The EI_{30} index is used to represent raindrop impact and surface runoff capacity to generate soil losses when all other erosion parameters are held constant (RENARD et al. 1997). The index is computed for individual rainstorms as the product of a storm's total kinetic energy (E) (MJ ha^{-1} mm^{-1}) times the storm's maximum 30 minute intensity (mm h^{-1}) (FOSTER et al., 1981). The R factor for RULSE is calculated as the sum of EI_{30} values over a specific time period (WISCHMEIER & SMITH, 1978; RENARD et al., 1997).

Since EI_{30} computation requires rather detailed, not always available data, equations linking rainfall coefficients – such as the Fournier index – to EI_{30} values have been developed for different locations (LAZZARI et al., 2015; MELLO et al., 2007). In this study, we have used the equation proposed by Aquino et al. (2014) for Lavras, a city northwest of the Upper Grande River basin:

$$EI_{30} = 85.672 * Rc^{0.6557} \quad (2)$$

$$Rc = \frac{p^2}{P} \quad (3)$$

where: Rc is Fournier's rainfall coefficient (mm); p is average monthly rainfall (mm) and P is average annual rainfall (mm).

In order to spatially represent the R factor, average monthly and annual rainfall layers were obtained from the WorldClim database (Figure 2a)

(HIJMANS et al., 2005). WorldClim provides climate grids interpolated from various weather stations, using data comprised between the years of 1950 to 2000 (HIJMANS et al., 2005). The rainfall grids were clipped within the study area and resampled to a 30 m grid cell resolution. Equation 2 was applied to the monthly rainfall layers, and the sum of resulting grids was calculated to represent average annual EI_{30}, i.e. the R factor for the Upper Grande River basin.

Soil erodibility factor (K)

Conceptually, soil erodibility expresses the propensity of a soil to suffer particle detachment by raindrop impact and surface runoff (RENARD et al, 1997). It is therefore influenced by a number of soil properties, such as hydraulic conductivity, surface roughness, soil texture and mineralogy. Quantitatively, the K factor is the rate of soil loss per erosion index unit as measured in a unit plot (22.13 m long, 9% slope, plowed downslope and kept continuously fallow) (WISCHMEIER & SMITH, 1978).

In this study, K factor values were taken from the available scientific literature (Table 1). All of the chosen factors were calibrated for Brazilian soils and priority was given to the factors obtained from plot based, natural rainfall experiments.

Table 1 Soil classes and respective soil erodibility (K factor) values

Soil Class	K factor	Source
	(t ha h ha^{-1} MJ^{-1} mm^{-1})	
AR	0.0000	-
CH	0.0105	Bertol et al. (2002)
CX	0.0355	Silva et al. (2009)
LA	0.0090	Silva et al. (2000)
LV	0.0032	Silva et al. (2009)
LVA	0.0100	Silva et al. (2000)

Table 1 Conclusion

PV	0.0320	Marques et al. (1997)
PVA	0.0106	Eduardo et al. (2013)
RL	0.0567	Castro et al. (2011)

Legend: AR: Rock outcrop; CH: Humic Cambisol; CX: Haplic Cambisol; LA: Yellow Latosol; LV: Red Latosol; LVA: Red Yellow Latosol; PV: Red Argisol; PVA: Red Yellow Argisol; RL: Litholic Neosol

The soil map of the State of Minas Gerais was used to assign K factor values according to the soil classes existing in the Upper Grande River Basin (Figure 2b) (FEAM, 2010). The soil map shapefile was converted into a 30 m resolution raster, where grid cell values represented soil erodibility.

Topographic factor (LS)

The topographic factor in USLE and RUSLE expresses the influence of slope length (L) and slope angle (S) on soil erosion. These parameters, however, are not easily determined at catchment scale, under non-uniform slopes and complex geomorphologic situations (RODRIGUEZ; SUAREZ, 2012).

In an attempt to improve USLE/RULSE application at natural landscape scenarios, Mitasova et al. (1996) proposed an equation for estimating the LS factor through GIS, following the concept of upslope contributing area introduced by Moore and Burch (1986) as a replacement for the slope length parameter:

$$LS = (m+1) * \left(\frac{U}{22.13}\right)^{m} * \left(\frac{\sin\theta}{0.0896}\right)^{n} \quad (4)$$

where: U (m^2m^{-1}) is the upslope contributing area per contour width (or cell resolution); θ is slope angle; m and n are empirical parameters that range

from 0.04 – 0.6 and 1.0 – 1.4, respectively, depending on the prevailing type of erosion (sheet or rill).

The use of upslope contributing area for the computation of the LS factor provides a spatial identification of flow convergence, which yields higher erosion predictions as flow concentration increases (MITASOVA et al., 2013). However, USLE and RULSE presuppose detachment capacity limited erosion, i.e. transport capacity exceeds detachment capacity everywhere (MITASOVA et al., 1996). In this case, deposition is not accounted for and, therefore, depositional areas should be identified and discarded from the analysis (MITASOVA et al., 2013). According to Fernandez et al. (2003), an upslope contributing area limit should be imposed to represent the depositional zones, or the areas where slope length becomes long and deposition occurs. Fernandez et al. (2003) and Yang et al. (2012) have suggested a value of 120 m.

In this study, the LS factor was calculated according to Equation 4, using ArcGIS 10.1 map algebra tools (ESRI, 2011). Parameters *m* and *n* where set as 0.4 and 1.0, respectively. Slope angle (θ) was derived from a 30 m resolution DEM obtained from SRTM (Shuffle Radar Topography Mission) imagery (Figure 1c). Upslope contributing area (U) was determined by further DEM processing: TauDEM 5.1.2 toolset (TARBOTON, 2014) for ArcGIS 10.1 (ESRI, 2011) was used to calculate upslope contributing area based on a D∞ flow direction algorithm (TARBOTON, 1997). A conservative limit of 360 m was set for maximum upslope contributing area per contour width.

Cover-management factor (C)

The C factor expresses the weighted ratio of soil losses on a given land use situation in relation to the ones measured in a unit plot (RENARD et al., 1997). Therefore, it reflects not only land cover, but also crop type, tillage

practices and other management conditions (PANAGOS et al., 2015b). C factor values typically range from 0 to 1.0. Low values are associated with densely vegetated landscapes, such as forested areas, and higher values relate to bare, fallow soils.

For erosion modeling at catchment scale, C factor values from the scientific literature can be assigned to uniform land use classes (PANAGOS et al., 2015b). In this study, land cover maps were produced using Landsat 8 Surface Reflectance images, dated from 2013 (Figure 2c). An object-oriented classification was performed using a fuzzy rule-based approach, through eCognition Developer software (TRIMBLE, 2010). Finally, C factor values were appointed to the 8 identified land use classes (Table 2).

Table 2 Land uses and respective C factor values

Land use	C factor	Source
Agriculture	0.156	De Maria; Lombardi Neto (1997)
Bare soil	1.000	Wischmeier; Smith (1978)
Eucalypt	0.124	Silva (2015)
Forest	0.016	Silva (2015)
Rangeland	0.025	Dedecek; Resck; Freitas (1986)
Ruspestrian vegetation	0.025	Dedecek; Resck; Freitas (1986)
Urban area	0.004	Fu; Chen; McCool (2006)

Support practice factor (P)

Field observation of the Upper Grande River Basin showed no consistent soil conservation practices. Although some contour tillage/seeding practices can be found on more technified agricultural areas, these proceedings are rare and can hardly be identified, given the large study area and the coarse

available satellite imagery. Therefore, a single P factor value of 1.0 was assigned to all the study area.

SEDD modeling

In the SEDD model, SDR_i expresses the probability that eroded particles, on a given upland location, will reach the nearest stream channel (FERRO; MINACAPILLI, 1995). SDR_i values range from 0 to 1.0, which quantify the percentage of gross erosion that is delivered to the stream network, and eventually, to the catchment outlet, since the model neglects channel deposition. This study used SEDD equations in a grid based methodology proposed by Jain and Kothyari (2000):

$$SDR_i = \exp(-\beta\, t_i) \tag{5}$$

where: SDR_i is the soil delivery ratio of a grid cell i; β is a catchment specific parameter and t_i is the overland flow travel time (h) from a grid cell i to the nearest stream channel along the flow path.

Overland flow travel time from a grid cell to the nearest stream channel along the flow path was computed as:

$$t_i = \frac{l_i}{v_i} \tag{6}$$

where: l_i is the flow length from cell i to the nearest stream channel (m) and v_i is the flow velocity for cell i (m s^{-1}).

The flow length parameter for equation 6 was calculated using the D8 Distance to Streams function of the TauDEM 5.1.2 (TARBOTON, 2014) toolset for ArcGIS 10.1 (ESRI, 2011). By inputting a DEM derived flow path grid and stream network grid, the algorithm computes the horizontal distance to streams, moving downslope according to the flow path.

Flow velocity was calculated observing Jain and Kothyari (2000), which incorporated the US Soil Conservation Service equation for overland and shallow channel flow (SCS, 1975) to the SEED model:

$$v_i = a_i S_i^{0.5} \quad (7)$$

where: a_i is a surface roughness coefficient for cell i (m s^{-1}) and Si is the slope for cell i (m m^{-1}).

As the a_i coefficient for equation 7 is dependent on land cover, values were assigned according to the land use map (Table 3).

Table 3 Values of a_i. Adapted from Haan, Barfield and Hayes (1994)

Land use	*a*
Agriculture	2.62
Bare soil	3.08
Eucalpyt	1.56
Forest	0.76
Rangeland	0.76
Ruspestrian vegetation	0.76
Urban area	6.19

Specific sediment yield (SSY_i) (t ha^{-1} yr^{-1}) quantifies the area specific amount of eroded sediment that reaches the catchment outlet. It can be determined as (JAIN; KOTHYARI, 2000):

$$SSY_i = SDR_i A_i \quad (8)$$

where: SSY_i is the specific sediment yield for a grid cell *i*; SDR_i is the soil delivery ratio for a grid cell *i* and A_i is the annual soil loss computed by RUSLE for a grid cell *i*.

The sediment yield (SY) (t yr^{-1}) of a river basin is estimated by multiplying the mean modeled SSY_i values by catchment area. In places where gauging stations provide measurements of river water sediment concentration, both SSY and SY can be directly estimated (WALLING, 1994). These measurements are used to calibrate and evaluate model forecasts (JETTEN; MANETA, 2011).

Measured sediment yield

The Brazilian National Water Agency (ANA) supplies data from a number of river gauging stations. Although daily discharge data is commonly assessed at these stations, total solids in the water are rarely measured. Even so, these measurements are sparse and often discontinuous. During the present research, the Funil hydroelectric power plant provided the only recent and continuous information on the total solids in the water within the Upper Grande river Basin. The data was collected at a gauging station in the Mortes River, at the Ibituruna municipality, upstream from the Funil reservoir. Suspended and bottom sediment concentration, as well as water discharge, were monthly evaluated from March 2008 to April 2012. This data was used to plot a

discharge curve, which related total sediments in the water (mg L^{-1}) to river discharge (m^3 s^{-1}) (Figure 3). Daily discharge values for the same gauging station, obtained from the ANA database, were applied to the discharge curve in order to better represent the variation of discharge and sediment transport during a longer period of time. Average annual SY was then calculated, as well as the SSY for the gauging station catchment area.

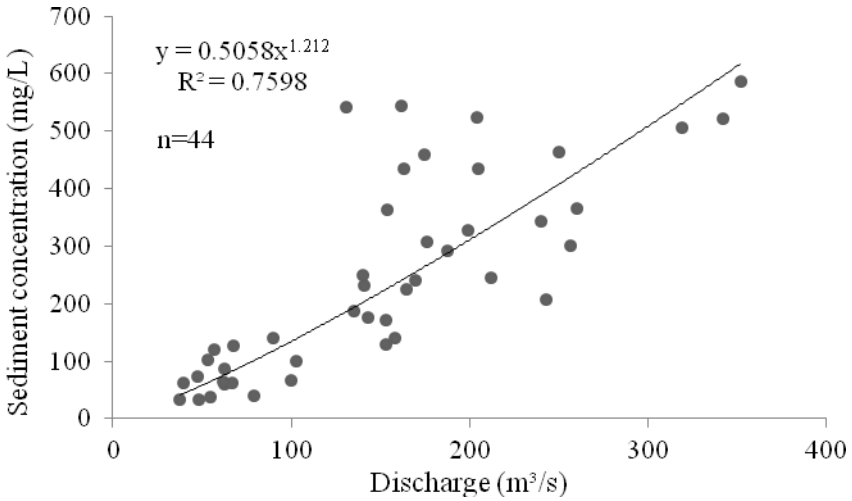

Figure 3 Discharge curve for the Mortes River at the Ibituruna gauging station

Model calibration

According to Ferro and Porto (2000), the catchment specific coefficient β for equation 5 lumps the spatial effects of roughness and runoff along the hydraulic flow path, also varying at a temporal scale. Although the authors suggested some deductive approaches for determining β at event scale, the coefficient has been generally calibrated by some sort of inverse modeling, i.e. by adjusting the parameter to best fit the observed SY values (FERNANDEZ et

al., 2003; FU; CHEN; MCCOOL, 2006; YANG et al., 2012; CHEN et al., 2016).

In this study, β was calibrated using measured sediment data from the Ibituruna gauging station. The catchment area of the station site was derived from the DEM, using ArcGIS 10.1 (ESRI, 2011) hydrology tools. As the station was close to the Mortes River mouth, catchment area (6040 km²) was similar to the area of Mortes River sub-basin (6243 km²). The best adjustment for β was found by comparing the SSY values obtained from the discharge curve to the mean SSY_i values estimated by the model within the gauging station catchment area (equation 8). The best-fit value of β was then applied to the SEDD equations in the whole Upper Grande River Basin.

RESULTS AND DISCUSSION

RUSLE model

Annual rainfall erosivity in the Upper Grande River Basin ranged from 5,193 to 7,027 MJ mm ha^{-1} h^{-1} yr^{-1}, with an average of 5,546 MJ mm ha^{-1} h^{-1} yr^{-1}. Such values are in agreement with the ones determined for the south of the State of Minas Gerais by Aquino et al. (2012), which ranged from 5,145 to 7,776 MJ mm ha^{-1} h^{-1} yr^{-1}. Spatially, greater erosivity was associated with higher elevation. The Mantiqueira mountain range, in the southern region of the study area, presented the highest values of rainfall erosivity (Figure 4a).

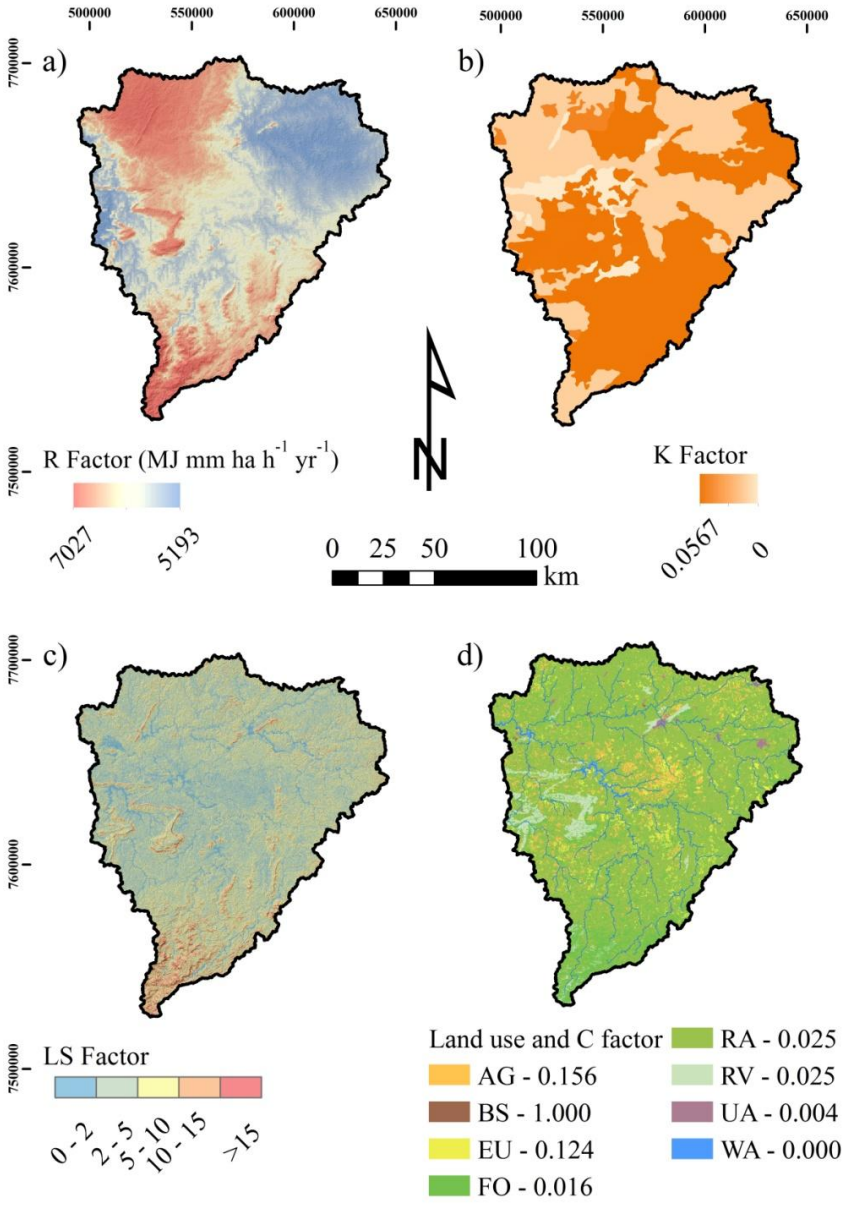

Figure 4 Layers of the RUSLE factors for the Upper Grande River Basin: R factor (a), K factor (b), LS factor (c) and C factor (d). Legend: AG: Agriculture; BS: Bare Soil; EU: Eucalypt; FO: Forrest; RA: Rangeland; RV: Rupestrian Vegetation; UA: Urban area; WA: Water

Red Yellow Latosols compose most of the northern section of the Upper Grande River Basin, whereas Haplic Cambisols are widespread on the southern and eastern portions. This soil class distribution meant lower K factor values within the Mortes River sub-basin when compared to the Grande River sub-basin. Most of the Litholic Neosols in the study area are mapped within the Capivari River sub-basin. These soils are very shallow and coarsely textured, which contributes to increase the erosion propensity in the subwatershed (Figure 4b).

The calculated LS factor varied from 0, in the very flat valleys where slope angle was null, to 43.74, at the steep hillslopes and flow convergence areas (Figure 4c). The average value was of 4.99.

The land use map revealed the prevalence of rangeland in the Upper Grande River Basin (Table 4) (Figure 4d). The area is mostly comprised of native pastures dedicated to dairy cattle raising, and characterized by low technological management systems (MENEZES et al., 2009).

Table 4 Land use in the Upper Grande River Basin

Land use	Area	
	km²	%
Agriculture	869	5.5
Bare soil	24	0.2
Eucalypt	741	4.7
Forest	4022	25.6
Rangeland	9277	59.1
Rupestrian vegetation	550	3.5
Urban area	94	0.6
Water	126	0.8

RUSLE predictions of average annual soil losses for the Upper Grande River Basin were of 22.35 t ha^{-1} yr^{-1} (Figure 5). Rangelands, the main land use in the study area, presented average soil losses of 16.63 t ha^{-1} yr^{-1}. Many pastures found in the basin are degraded, and therefore, may experience greater erosion than well-managed rangelands. Also, during the beginning of the rainy season, pastures are usually sparsely vegetated as a result of overgrazing and the lack of rainfall during the winter. Therefore, the single C factor value appointed to such land use might not represent the spatial and temporal variability of the parameter, which associates uncertainty to the model predictions.

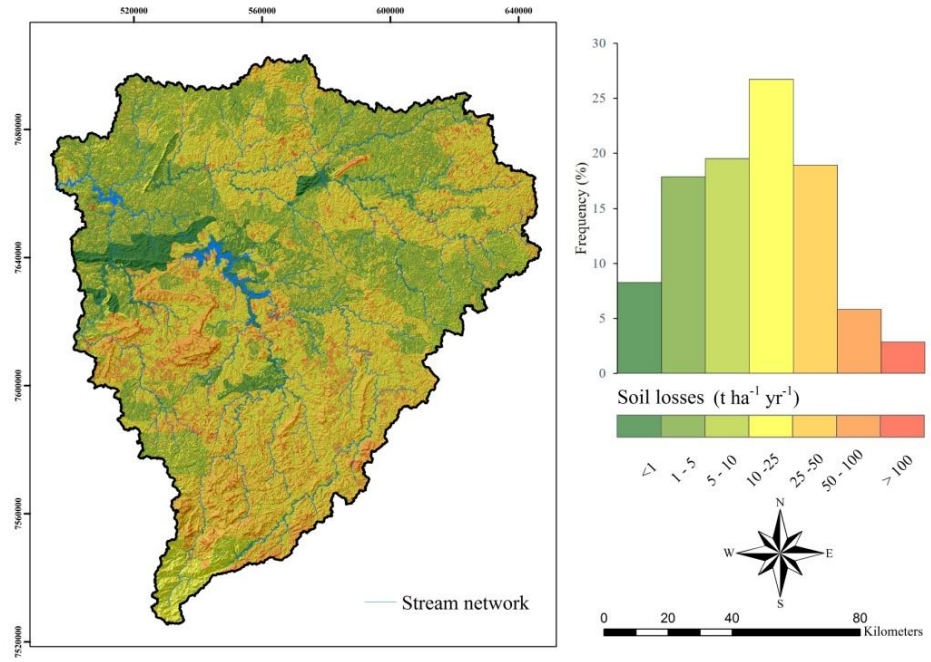

Figure 5 Average annual soil losses in the Upper Grande River Basin

Although the same C factor value was assigned to rangeland and rupestrian vegetation, RUSLE estimations, in the latter case, showcased 33.25 t ha^{-1} yr^{-1} average soil losses. That stems from the fact that rupestrian vegetation is

strongly associated with ridge formations and Litholic Neosols, the most erodible soil class in the basin (Table 5).

Table 5 Soil class percentage distribution among the land use classes in the Upper Grande River Basin

	Land Use						
Soil Class	AG	BS	EU	FO	RA	RV	UA
	---------- % ----------						
CH	00.05	01.64	00.17	07.09	00.78	10.50	00.16
CX	29.76	40.98	43.94	47.12	48.33	18.87	48.66
LA	00.09	00.00	01.16	00.28	00.61	00.00	00.00
LV	06.16	01.58	02.42	01.54	02.15	00.88	01.78
LVA	52.19	31.13	37.73	25.83	32.73	13.58	38.52
PV	00.77	00.37	01.30	02.40	02.98	00.12	00.26
PVA	06.23	10.56	07.42	07.19	07.59	01.52	08.87
RL	04.74	13.75	05.87	08.56	04.83	54.53	01.74

Legend: CH: Humic Cambisol; CX: Haplic Cambisol; LA: Yellow Latosol; LV: Red Latosol; LVA: Red Yellow Latosol; PV: Red Argisol; PVA: Red Yellow Argisol; RL: Litholic Neosol; AG: Agriculure; BS: Bare soil; EU: Eucalypt; FO: Forest; RA: Rangeland; RV: Rupestrian vegetation; UA: Urban area

Gross erosion predictions for forest areas of 16.21 t ha^{-1} yr^{-1} were higher than the usual USLE/RULSE estimations for such land use in Brazilian watersheds (AVANZI et al., 2013; SILVA, 2015). As reminiscent forests in the Upper Grande River Basin are mostly located on drainage lines and very steep slopes, which are improper for agriculture or grazing, the model depicted a great propensity to soil erosion. The mean LS factor value for forests was 33% and 94% higher than the ones for rangeland and agriculture, respectively. It is pertinent to point out that although soil losses on cultivated lands have a strong relation to slope length and slope angle, the same cannot be confirmed for dense, naturally vegetated areas, where hydraulic conductivity is high and extremely

variable (GOVERS, 2011). Therefore, RUSLE predictions of erosion rates for forests may be overestimated in this study.

The average soil losses for eucalypt and agriculture were of 65.93 and 57.29 t ha^{-1} yr^{-1}, respectively, in spite of the greater C factor assigned to croplands. In the Upper Grande River Basin, agricultural areas are mainly located where less erodible soils occur; that means 59% of the croplands were found on Latosols, whereas eucalypt was mainly associated with Haplic Cambisols. Moreover, in comparison to croplands, eucalypt forests had a greater area located on other highly erodible soils (Table 5). Also, agriculture tends to be established on smooth landscapes, more suited to mechanization. Mean values of the LS factor for croplands were 17% lower than those of eucalypt forests. As stated by Silva et al. (2014), eucalypt plantations in Brazil are often situated in vulnerable ecosystems, on previously degraded areas with steep slopes and highly erodible soils.

The estimated soil losses for urban areas were the lowest among the land uses: 2.14 t ha^{-1} yr^{-1}. In contrast, the highest erosion predictions were associated with bare soils, where average soil losses were of 604.58 t ha^{-1} yr^{-1}. In the study area, bare soils consisted of fallow and degraded soils, as well as strip mines and unpaved roads.

Regarding the gross erosion rates on the three main subwatersheds of the study area, RUSLE predicted soil losses of 26.97, 26.18 and 16.81 t ha^{-1} yr^{-1} for the Capivari River, the Grande River and the Mortes River sub-basins, respectively. Land use distribution and rainfall erosivity were found to be rather similar among the subwatersheds. Therefore, the contrast of erosion intensity can be explained by the variation of topography and, primarily, of soil erodibility, as mentioned before.

SEDD model

Measured data and model calibration

According to the discharge curve for the Ibituruna gauging station, the average annual SSY in the Mortes River Basin was of 1.60 t ha^{-1} yr^{-1}, with a 2.9 % coefficient of variation (CV). Correlation analysis between monthly rainfall erosivity and SSY showed a coefficient of determination of 73%. However, monthly SSY did not increase directly with erosivity, given that eroded sediments do not reach the catchment outlet immediately, and are remobilized several times before being discharged. During the end of the rainy season, in April, although rainfall erosivity declines, SSY is still significant. Such behavior is possibly explained by the fact that previously eroded particles continue to be transported by the stream network (Figure 6).

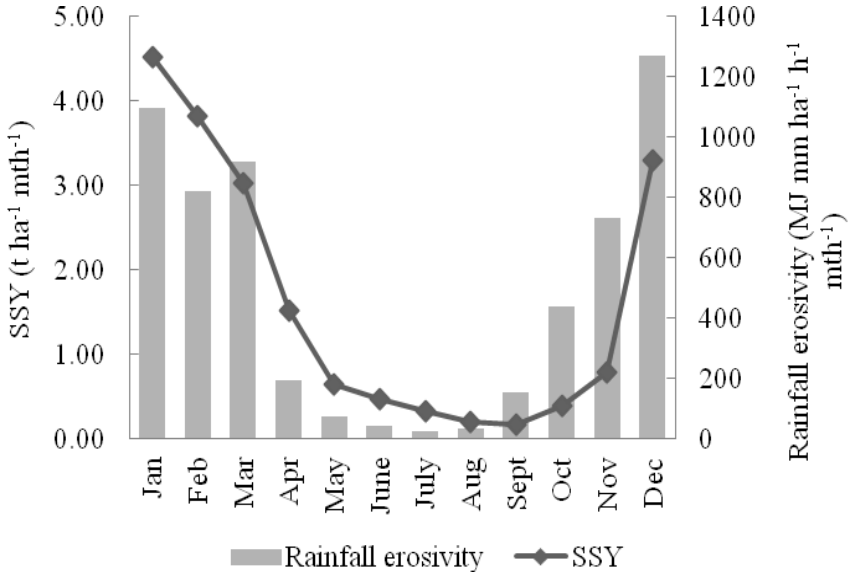

Figure 6 Average monthly SSY and rainfall erosivity for the Mortes River sub-basin, upstream from the Ibituruna gauging station

Calibration of the β coefficient for the SEDD equation indicated that the model was sensitive to the parameter. Average modeled SSY_i for the Mortes River sub-basin varied 58% as β ranged from 1.0 to 4.0. By setting the β parameter to 3.0, SEDD predictions yielded a mean SSY_i value of 1.58 t ha^{-1} yr^{-1}, which resulted in an error of 0.02 t ha^{-1} yr^{-1}, or 1.25%.

It is important to highlight that the β parameter may be a source of great uncertainty in the SEDD model. The user is able to achieve practically any result by varying this basin-specific coefficient. Uncertainty and sensitivity analysis should be employed to verify the model's prediction capacity, as performed by Stefano and Ferro (2007). However, the lack of proper validation data in the study area hampered such investigation. Nevertheless, the calibrated β value in this study was similar to the ones reported by Yang et al. (2012). According to the authors, the best SEDD model results for two river basins, with 4500 and 7140 km², were obtained with β values of 3.2 and 4.6, respectively. According to Lin et al. (2016), the calibrated β value for a watershed with 486 km² in China was of 0.304; whereas Fu, Chen and McCool (2006) reported that a β of 1.0 yielded the best predictions of SSY for a 327 km² watershed. Hence, although β theoretically lumps the effects of roughness and runoff along the hydraulic path, the coefficient seems to have some empirical relation with catchment area. According to equation 5, SDR_i will decrease as β increases. As the highest reported β values relate to larger watersheds, and SDR overall tends to decrease with catchment area (WALLING, 1994), it is to be expected that calibrated β values will generally increase with watershed size.

Sediment Delivery Ratio, Specific Sediment Yield and Total Sediment Yield

Once the β coefficient was calibrated for the Mortes River sub-basin, the best-fit value of 3.0 was applied to the Upper Grande River Basin, which resulted in the SDR_i layer displayed in Figure 7a.

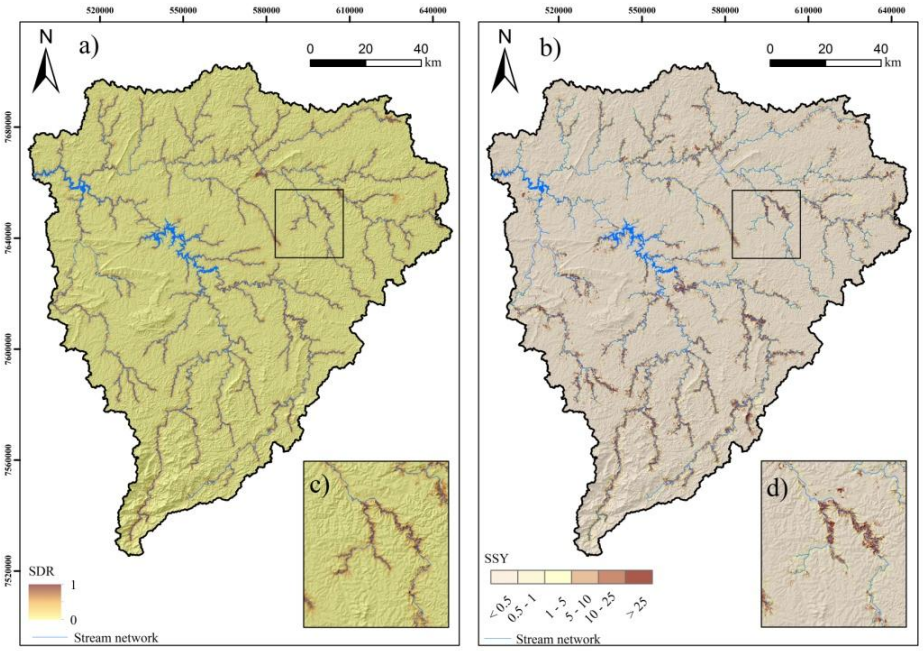

Figure 7 Sediment delivery rate (a) (c) and specific sediment yield (b) (d) in the Upper Grande River Basin

The mean value of SDR_i for the study area was of 0.07. The spatial distribution of SDR_i indicates that the sediment sources closer to the stream channels have higher probability of delivering eroded particles to the water courses. However predicable this might look, flow velocity, which depends on slope gradient and surface roughness, is used in the SEDD model as a proxy for overland flow transport capacity. Therefore, wherever flow velocity is high, eroded particles have a greater possibility of being transported to the stream network as opposed to being deposited along the hillslopes. As surface

roughness was determined according to land use, predictions of SDR_i were influenced by such parameter (Table 6).

Table 6 SDR_i values according to the different land uses in the Upper Grande River Basin

Land use	SDR_i	
	Mean	Coefficient of variation (%)
Agriculture	0.13	60.12
Bare soil	0.16	72.78
Eucalypt	0.09	49.93
Forest	0.06	36.00
Rangeland	0.06	37.86
Rupestrian vegetation	0.03	26.32
Urban area	0.43	140.67

Correlation analysis between surface roughness (parameter *a* of equation 7) and mean SDR_i values for the land use classes showed a coefficient of determination of 97%. These results differ from the ones of Fernandez et al. (2003) and Fu, Chen and McCool (2006), in which SDR_i did not exhibit a clear relation with land use.

Since parameter *a* is constant for a specific land use, the CV of SDR_i reflects the spatial variability of the distance to streams and slope gradient. Land uses with very specific geographical distribution, such as the rupestrian vegetation, had a lower variability of SDR_i. On the other hand, the high CV for urban areas demonstrates that such land use does not have an obvious geographical pattern concerning slope and proximity to water courses (Table 6).

The average SSY_i in the Upper Grande River was of 1.93 t ha^{-1} yr^{-1} (Figure 7b). The distance to streams did not influence SSY_i values as much as it influenced SDR_i. The zoom-in data frames in Figures 7c and 7d demonstrate

how SSY_i varies within a close distance to the stream channel. Such behavior is expected since SSY_i depends on the gross erosion rates. This means that, even if a given sediment source is closely located to the stream network, and transport capacity of the overland flow is high, SSY_i will not be expressive if particle detachment is low.

According to the SEDD model predictions, bare soils had the highest average SSY_i among the land uses of the study area (Table 7). These results are connected to the extremely high erosion rates predicted by RULSE in such land use class. Also, the average values of SDR_i for bare soils indicated a greater propensity of sediment delivery to streams in comparison to other land uses. Bare soils comprise 0.16% of the study area. However, the model estimated that almost 9% of the total SY in the Upper Grande River basin originates from fallow or degraded soils, strip mines and unpaved roads (Table 7).

Agriculture produced the second highest SSY_i values. Although croplands comprise only 5.5% of the study area, such land use generated 25% of the total SY in the basin. Eucalypt forests also showed expressive SSY_i values, which were only lower than the ones for bare soils and agriculture (Table 7). Rangeland and forests which, combined, occupy 85% of the Upper Grande River Basin account for only 46% of the total SY. Therefore, according to the model predictions, sediment production in the study area is much influenced by intensive land use.

Table 7 Mean SSY_i, SY and percentage of SY according to the land use classes in the Upper Grande River Basin

Land use	SSY_i	SY	
	t ha^{-1} yr^{-1}	t yr^{-1}	%
Agriculture	8.82	767,370	25.3
Bare soil	110.94	268,831	08.9

Table 7 Conclusion

Eucalypt	7.21	534,885	17.7
Forest	0.91	368,066	12.1
Rangeland	1.12	1,040,978	34.3
Rupestrian vegetation	0.77	42,670	01.4
Urban area	0.83	8,265	0.27

Since the SEDD model neglects channel deposition, it is assumed that all sediments that reach the stream network will be discharged through the river basin outlet. In the Grande River sub-basin, upstream from the Camargos /Itutinga reservoir, average values of SSY_i were of 2.32 t ha^{-1} yr^{-1}. Therefore 1.45 million t yr^{-1} of sediments are delivered into the reservoir, considering a catchment area of 624,300 ha. These results differ from the ones presented by Beskow et al. (2009). According to these authors, SSY upstream from the reservoir was of 0.81 t ha^{-1} yr^{-1}. Although these estimations were based on river gauging station data, they may not be representative of current conditions, since the information was comprised between 1996 and 2003. Also, in the same study, river sediment concentration was only evaluated 5 times per year, not allowing sediment transport dynamics to be properly represented. However, given the lack of recent sediment measurements upstream from the Camargos/Itutinga reservoir, the SEDD model could not be calibrated; hence, the SSY_i results from this study should be analyzed with caution.

The catchment area of the Funil power plant reservoir consists in the whole Upper Grande River Basin. Since most of the sediments generated upstream from the Camargos/Itutinga reservoir are retained in the dam, we assumed that the drainage area of the Funil reservoir consisted of the following subwatersheds: the Capivari River sub-basin, the Mortes River sub-basin and the

portion of the Grande River sub-basin located downstream from the Camargos/Itutinga reservoir.

The SEDD model predictions indicated that the primary source of sediments in the Funil reservoir is the Mortes River, which delivers 1.04 million t yr^{-1} of sediments into the reservoir. According to recent bathymetric surveys, the Mortes River delta is the main sedimentation zone in the Funil reservoir (SOARES 2015). Navigation is already hampered in the shallow delta waters, given the amount of deposited sediments.

The average SSY_i values in the Capivari River sub-basin was of 2.34 t ha^{-1} yr^{-1}. The river drains an area of 207,800 ha, which transports a total of 486,960 t yr^{-1} of sediments into the Funil reservoir. Considering only the drainage area downstream from the Itutinga/Camargos reservoir, the Grande River transports 56,804 t yr^{-1} of sediments.

Therefore, the modeling results indicate that sediment delivery to the Funil reservoir is of 1.59 million t yr^{-1}. Based on the results from bathymetric surveys in the reservoir, the annual loss of storage capacity due to sedimentation is estimated as 2.8 million m^3 (SOARES, 2015). Since bulk density of the bottom sediments in the reservoir could not be evaluated, a comparison between the model predictions and the sediment deposition could not be properly done. Nevertheless, considering these values, it seems reasonable to state that RUSLE and SEDD underestimated the amount of sediments that reach the Funil reservoir annually. If we accept such premise, the poor performance of the model may be explained mainly by two factors: firstly, RULSE soil loss estimations do not represent the erosion dynamics in permanent gullies, river bank erosion, and landslides, which may be a significant source of sediments in river basins (VERSTRAETEN et al., 2003). Secondly, the assumption made in the present study that the Camargos/Itutinga reservoir retains all sediments

eroded upstream may be imprecise due to the fact that reservoirs are unlikely to present 100% trapping efficiency, i.e. part of the sediments that reach a reservoir is likely to transpose the dam (Jain and Singh, 2003). In order to determine trapping efficiency, it would be necessary to have very detailed sediment sampling, upstream and downstream from the Carmargos/Itutinga reservoir; however, given the lack of operating river gauging stations in the study area, such data was not available. It is important to point out that although reservoir bathymetric surveys supply the most accurate estimations of river basins SY, such evaluations are not free from errors (VERSTRAETEN et al, 2003; DE VENTE et al., 2013). In the case of the Funil reservoir, the recent work of Soares (2015) is based on very densely sampled bathymetric surveys. Previous surveys in the area, however, were not as detailed, and the reservoir storage capacity might not have been precisely estimated.

CONCLUSIONS

In the Upper Grande River Basin, bare soils, eucalypt forests and agriculture presented the highest soil losses among the identified land cover classes, according to the RUSLE predictions. Therefore, soil conservation planning should focus on these land uses, and eucalypt forests should receive special attention. The model predictions demonstrated that, in the study area, eucalypts are located on steep hillslopes with erosion-prone soils, and experience severe soil losses.

The results from the SEDD model indicated that, within the identified land uses classes, rangelands are the main source of sediments in Upper Grande River Basin. However, that stems from the fact that pastures comprise most of the study area. Bare soils, agriculture and eucalypt presented the highest area-specific sediment yield values. Such land uses generate a great amount of sediment within relatively small areas. Hence, in order to reduce the off-site

erosion impacts in the basin, soil management support practices on croplands and eucalypt forests should be widely encouraged. Moreover, the identification and rehabilitation of degraded bare soils may further decrease the sediment yield in the basin.

Also according to the SEDD model results, sedimentation in the Funil reservoir is mostly linked to sediments transported by the Mortes River. These results are corroborated by field observation and recent bathymetric surveys. The Camargos/Itutinga reservoir receives a similar annual sediment input as does the Funil reservoir. However, the latter may experience greater sedimentation rates due to its lower storage capacity. Given the relevance of the Upper Grande River Basin in generating hydroelectric power, the monitoring of sediment fluxes into the basin's main reservoirs should be intensified.

It is important to point out that the results provided by this study are an initial estimation of the erosion and sediment delivery dynamics in the Upper Grande River Basin. Field data must be gathered in order to verify the quantity and the sources of sediments that reach the water courses. Although the modeling results from this study have been successfully calibrated, much uncertainty can be associated to the predictions. A model may accurately predict the sediment yield from a river basin without actually being "correct", especially when calibration from observed data is employed. In the case of the SEDD model, the basin-specific coefficient β strongly increases the user's degree of freedom, and also, the uncertainty of the predictions. The validation of erosion prediction models is somewhat problematic, given the spatial and temporal variability of the phenomenon. Nevertheless, validation efforts should be increased, especially when models are applied in situations for which they were not developed. A more robust validation dataset must be gathered in order to properly evaluate the performance of the RULSE/SEDD modeling under

tropical conditions. Initial results, however, indicate that the approach may be useful for analyzing sediment transport in Brazilian watersheds, where limited input data is available.

REFERENCES

AKSOY, H.; KAVVAS, M. L. A review of hillslope and watershed scale erosion and sediment transport models. **Catena**, v. 64, p. 247–271, 2005.

ALVARES, C. A.; STAPE, J. L.; SENTELHAS, P. C.; GONÇALVES, J. L. M.; SPAROVEK, G. Köppen's climate classification map for Brazil. **Meteorologische Zeitschrift**, v. 22, n. 6, p. 711–728, 2013.

AQUINO, F.; SILVA, M. L. N.; FREITAS, D. A. F.; CURI, N.; MELLO, C. R.; AVANZI, J. C. Erosividade das chuvas e tempo de recorrência para Lavras , Minas Gerais. **Ceres**, v. 61, n.1, 2014.

AQUINO, R. F.; SILVA, M. L. N.; FREITAS, D. A. F.; CURI, N.; MELLO, C. R.; AVANZI, J. C. Spatial variability of the rainfall erosivity in southern region of Minas Gerais state, Brazil. **Ciência e agrotecnologia**, v. 36, n. 5, p. 533–542, 2012.

AVANZI, J. C.; SILVA, M. L. N.; CURI, N.; NORTON, L. D.; BESKOW, S.; MARTINS, S. G. Erosion with eucalyptus and atlantic forest. **Ciência e agrotecnologia**, v.37, n. 5, p. 427–434, 2013.

BERTOL, I.; SCHICK, J.; BATISTELA, O.; LEITE, D.; AMARAL, A. J. Erodibilidade de um Cambissolo Húmico alumínico léptico , determinada sob chuva natural entre 1989 e 1998 em Lages (SC). **Revista Brasileira de Ciência do Solo**, v. 36, p. 465–471, 2002.

BESKOW, S.; MELLO, C. R.; NORTON, L. D.; CURI, N.; VIOLA, M. R.; AVANZI, J. C. Soil erosion prediction in the Grande River Basin, Brazil using distributed modeling. **Catena**, v. 79, n. 1, p. 49–59, 2009.

BURTON, R. **Explorations of the Highlands of Brazil.** London: Tinsley Brothers, 443p. 1869.

CASTRO, W. J.; LEMKE-DE-CASTRO, M. L.; LIMA, J. O.; OLIVEIRA, L. F. C.; RODRIGUES, C.; FIGUEIREDO, C. C. Erodibilidade de solos do cerrado goiano. **Revista em Agronegócios e Meio Ambiente**, v.4, n.2, p. 305-320, 2011.

CHEN, L.; WU, Z.; MA, R.; SU, Z. Detection of sensitive soil properties related to non-point phosphorus pollution by integrated models of SEDD and PLOAD. **Ecological Indicators**, v. 60, p. 483-494, 2016.

SERVIÇO GEOLÓGICO DO BRASIL – CPRM. **Mapa geológico do estado de Minas Gerais**. Brasília: CPRM, 2003. Escala 1:1.000.000.

DEDECEK, R.A.; RESCK, D.V.S.; FREITAS, E. Perdas de solo, água e nutrients por erosão em Latossolo Vermelho-Escuro dos cerrados em diferentes cultivos sob chuva natural. **Revista Brasileira de Ciência do Solo**, v. 10, p. 265-272, 1986.

DE MARIA, I. C.; LOMBARDI NETO, F. Razão de perdas de solo e facor C para sistemas de manejo da cultura do milho. **Revista Brasileira de Ciência do Solo**, v. 21, p. 263-270, 1997.

DE VENTE, J.; POESEN, J.; VERSTRAETEN, G.; GOVERS, G.; VANMAERCKE, M.; VAN ROMPAEY, A.; ARABKHEDRI, M.; BOIX-FAYOS, C. Predicting soil erosion and sediment yield at regional scales: Where do we stand? **Earth-Science Reviews**, v. 127, p. 16–29, 2013.

DOTTERWEICH, M. The history of human-induced soil erosion: Geomorphic legacies, early descriptions and research, and the development of soil conservation—A global synopsis. **Geomorphology**, v. 201, p. 1–34, 2013.

EDUARDO, E. N.; CARVALHO, D. F.; MACHADO, R. L.; SOARES, P. F. C.; ALMEIDA, W. S. Erodibilidade, fatores cobertura e manejo e práticas conservacionistas em Argissolo Vermelho-Amarelo, sob condições de chuva natural. **Revista Brasileira de Ciência do Solo**, v.37, p. 796-803, 2013.

ENVIRONMENTAL SYSTEMS RESEARCH INSTITUTE – ESRI. ArcGIS for Desktop, version 10.1. Redlands, 2011. CD ROM.

FUNDAÇÃO ESTADUAL DO MEIO AMBIENTE – FEAM. **Mapa de solos de Minas Gerais:** legenda expandida. Belo Horizonte: FEAM/UFV/CETEC/UFLA, 2010. 40 p.

FERNANDEZ, C.; WU, J. Q.; MCCOOL, D. K.; STOCKLE, C. O. Estimating water erosion and sediment yield with GIs , RUSLE , and SEDD. **Journal of Soil and Water Conservation**, v. 58, p. 128–136, 2003.

FERRO, V.; MINACAPILLI, M. Sediment delivery processes at basin scale. **Hydrological Sciences Journal**, v. 40, n. 6, p. 703–717, 1995.

FERRO, V.; PORTO, P. Sediment Delivery Distributed (SEDD) Model. **Journal Of Hydrologic Engineering**, v. 5, n. 4, p. 411–422, 2000.

GOMIDE, P. H. O.; SILVA, M. L. N.; SOARES, C. R. F. S. Atributos físicos, químcos e biológicos do solo em ambientes de voçorocas no município de Lavras - MG. **Revista Brasileira de Ciência do Solo**, v. 35, p. 567–577, 2011.

GOVERS, G. Misapplications and misconceptions of erosion models. In: MORGAN, R. P. C.; NEARING, M. A. **Handbook of erosion modeling**. Oxford: Blackwell Publishing Ltd, 2011. p. 117-134.

HAAN, C. T.; BARFILED, B. J.; HAYES, J. C. **Design Hidrology and Sedimentology for Small Catchments**. San Diego: Academic Press, 1994. 588p.

HIJMANS, R. J.; CAMERON, S. E.; PARRA, J. L.; JONES, P. G.; JARVIS, A. Very high resolution interpolated climate surfaces for global land areas. **International Journal of Climatology**, v. 25, n. 15, p. 1965–1978, 2005.

HU, B.; YANG, Z.; WANG, H.; SUN, X.; BI, N.; LI, G. Sedimentation in the Three Gorges Dam and the future trend of Changjiang (Yangtze River) sediment flux to the sea. **Hidrology and Earth System Sciences**, v. 13, p. 2253–2264, 2009.

JAIN, M. K.; KOTHYARI, U. C. Estimation of soil erosion and sediment yield using GIS. **Hydrological Sciences Journal**, v. 45, n. 5, p. 771–786, 2000.

JAIN, S. K.; SINGH, V.P. **Water resources systems planning and management**. New York: Elsevier, 2003. 858p.

JETTEN, V. G.; MANETA, M. P. Calibration of erosion models. In: MORGAN, R. P. C.; NEARING, M. A. **Handbook of erosion modeling**. Oxford: Blackwell Publishing Ltd, 2011. p. 33-51.

LAZZARI, M.; GIOIA, D.; PICCARRETA, M.; DANESE, M.; LANORTE, A. Sediment yield and erosion rate estimation in the mountain catchments of the Camastra artificial reservoir (Southern Italy): A comparison between different empirical methods. **Catena**, v. 127, p. 323–339, 2015.

MARQUES, J. J. G. S. M.; CURI, N.; FERREIRA, M. M.; LIMA, J. M.; SILVA, M. L. N.; CAROLINO DE SÁ, M. A. Adequação de métodos indiretos para a estimativa de erodiblidade de solos com horizonte B textural no Brasil. **Revista Brasileira de Ciência do Solo**, v.21, p. 447-456, 1997.

MELLO, C. R.; SÁ, M. A. C.; CURI, N.; MELLO, J. C.; VIOLA, M. R.; SILVA, A. M. Erosividade mensal e anual da chuva no Estado de Minas Gerais. v. 30, n. 1, p. 537–545, 2007.

MENEZES, M. D.; CURI, N.; MARQUES, J. J.; MELLO, C. R.; ARAUJO, A. R. Levantamento pedológico e Sistema de Informações Geográficas na avaliação do uso das terras em sub-bacia hidrográfica de Minas Gerais. **Ciência e agrotecnologia**, v. 33, n. 6, p. 1544–1553, 2009.

MERRITT, W. S.; LETCHER, R. A.; JAKEMAN, A. J. A review of erosion and sediment transport models. **Environmental Modelling & Software**, v. 18, n. 8-9, p. 761–799, 2003.

MITASOVA, H.; HOFIERKA, J.; ZLOCHA, M; IVERSON, L. R.. Modeling topographic potential for erosion and deposition using GIS. **International Journal of Geographical Information Science,** v. 10, n. 5, p. 629-641, 1996.

MITASOVA, H.; BARTON, M.; HOFIERKA, J.; HARMON, R. S. GIS-Based Soil Erosion Modeling. In: SHRODER, J. F. **Treatise on Geomorphology**. San Diego: Academic Press, 2013. p. 228-258.

MOORE, I. D.; BURCH, G. J. Modeling erosion and deposition: Topographic effects. **Transactions ASAE**, n. 29, p. 1624-1640, 1986.

MORGAN, R. P. C. **Soil Erosion and Conservation**. 3rd ed. Oxford: Blackwell Publishing, 2005. 299 p.

OUYANG, W.; HAO, F.; SKIDMORE, A. K.; TOXOPEUS, A. G. Soil erosion and sediment yield and their relationships with vegetation cover in upper stream of the Yellow River. **The Science of the total environment**, v. 409, n. 2, p. 396–403, 2010.

PANAGOS, P.; BORRELLI, P.; MEUSBURGER, K.; ALEWELL, C.; LUGATO, E.; MONTANARELLA, L. Estimating the soil erosion cover-management factor at the European scale. **Land Use Policy**, v. 48, p. 38–50, 2015a.

PANAGOS, P.; BORRELLI, P.; POESEN, J.; BALLABIO, C.; LUGATO, E.; MEUSBURGER, K.; MONTANARELLA, L.; ALEWELL, C. The new assessment of soil loss by water erosion in Europe. **Environmental Science & Policy**, v. 54, p. 438–447, 2015b.

PIMENTEL, D. Soil Erosion: A Food and Environmental Threat. **Environment, Development and Sustainability**, v. 8, n. 1, p. 119–137, 2006.

POESEN, J. Challenges in gully erosion research. **Landform Analysis**, v. 17, p. 5–9, 2011.

RENARD, K. G.; FOSTER, G. R.; WEESIES, G. A.; MCCOOL, D. K.; YODER, D. C. **Predicting soil erosion by water: a guide to conservation planning with the Revised Universal Soil Loss Equation**. Washington: U.S. Department of Agriculture, 1997. 384p.

RENSCHLER, C. S.; HARBOR, J. Soil erosion assessment tools from point to regional scales—the role of geomorphologists in land management research and implementation. **Geomorphology**, v. 47, n. 2-4, p. 189–209, 2002.

RODRIGUEZ, J. L. G.; SUAREZ, M. C. G. Methodology for estimating the topographic factor LS of RUSLE3D and USPED using GIS. **Geomorphology**, v. 175-176, p. 98–106, 2012.

SILVA, M.L.N. Erosividade da chuva e proposição de modelos para estimar a erodibilidade de Latossolos brasileiros. 1997. 154 p. PhD thesis – Universidade Federal de Lavras, Lavras, 1997.

SILVA, M. L. N.; CURI, N.; LIMA, J. M.; FERREIRA, M. M. Avaliação de métodos indiretos de determinação da erodibilidade de Latossolos Brasileiros. **Pesquisa Agropecuária Brasileira**, v. 35, n. 6, p. 1207-1220, 2000.

SILVA, A. M.; SILVA, M. L. N.; CURI, N.; AVANZI, J. C.; FERREIRA, M. M. Erosividade da chuva e erodibilidade de Cambissolo e Latossolo na região de Lavras, sul de Minas Gerais. Revista Brasileira de Ciência do Solo, v. 33, n. 6, p. 1811-1820, 2009.

SILVA, M. A.; SILVA, M. L. N.; CURI, N.; OLIVEIRA, A. H.; AVANZI, J. C.; NORTON, L. D. Water erosion risk prediction in eucalyptus plantations. **Ciência e agroctenologia**, v. 38, n. 2 p. 160–172, 2014.

SILVA, B. P. C. **Medição e Modelagem da erosão hídrica em sub-bacia hidrográfica em sistemas florestais**. 2015. 120 p. MS Thesis – Universidade Federal de Lavras, Lavras, 2015.

SOARES, W. S. **Taxa de assoreamento no reservatório da Usina Hidrelétrica do Funil - MG.** 2015. 45p. MS Thesis – Universidade Federal de Lavras, Lavras, 2015.

STEFANO, C. DI; FERRO, V. Evaluation of the SEDD model for predicting sediment yield at the Sicilian experimental SPA2 basin. **Earth Surface Processes and Landforms,** v. 32, p. 1094–1109, 2007.

TAGUAS, E. V.; MORAL, C.; AYUSO, J. L.; PEREZ, R.; GOMEZ, J. A. Modeling the spatial distribution of water erosion within a Spanish olive orchard microcatchment using the SEDD model. **Geomorphology**, v. 133, n. 1-2, p. 47–56, 2011.

TANYAŞ, H.; KOLAT, Ç.; SÜZEN, M. L. A new approach to estimate cover-management factor of RUSLE and validation of RUSLE model in the watershed of Kartalkaya Dam. **Journal of Hydrology**, v. 528, p. 584–598, 2015.

TARBOTON, D. G. A new method for the determination of flow directions and upslope areas in grid elevation models. **Water Resources Research**, v. 33, n. 2, p. 309-319, 1997.

TARBOTON, D. G. TauDem 5.1.2: terrain analysis using digital elevation models. Available in: http://hydrology.usu.edu/taudem/taudem5/ downloads.html. Access on: august 15, 2014.

TRIMBLE. **eCognition® Developer 8.64.0 reference book**. 2010. Available at: http://www.definiens.com/. Access on may 11, 2015.

VANMAERCKE, M.; POESEN, J.; VERSTRAETEN, G.; DE VENTE, J.; OCAKOGLU, F. Sediment yield in Europe: Spatial patterns and scale dependency. **Geomorphology**, v. 130, n. 3-4, p. 142–161, 2011.

VERSTRAETEN, G.; POESEN, J.; DE VENT, J.; KONINCKX, X. Sediment yield variability in Spain: a quantitative and semiqualitative analysis using reservoir sedimentation rates. **Geomorphology**, v. 50, n. 4, p. 327–348, 2003.

WALLING, D. E. Measuring sediment yield from river basins. In: LAL, R. **Soil erosion research methods**. Washington: Soil and Water Conservation Society; 1994. p.39-82.

WISCHMEIER, W. H.; SMITH, D. D. **Predicting rainfall erosion losses**: **a guide to conservation planning**. Washington: USDA, 1978. 58 p.

WU, C.-H.; CHEN, C. N.; TSAI, C. H.; TSAI, C. T. Estimating sediment deposition volume in a reservoir using the physiographic soil erosion-deposition model. **International Journal of Sediment Research**, v. 27, n. 3, p. 362–377, 2012.

XIAOYING, L.; QI, S.; HUANG, Y.; CHEN, Y.; DU, P. Predictive modeling in sediment transportation across multiple spatial scales in the Jialing River Basin of China. **International Journal of Sediment Research**, v. 30, n. 3, 2015.

XU, L.; XU, X.; MENG, X. Risk assessment of soil erosion in different rainfall scenarios by RUSLE model coupled with Information Diffusion Model: A case study of Bohai Rim, China. **Catena**, v. 100, p. 74–82, 2013.

YANG, M.; LI, X.; HU, Y.; HE, X. Assessing effects of landscape pattern on sediment yield using sediment delivery distributed model and a landscape indicator. **Ecological Indicators**, v. 22, p. 38–52, 2012.

ARTIGO 2 - HYBRID KRIGING METHODS FOR INTERPOLATING SPARSE BATHYMETRY POINT DATA

ABSTRACT

Creating precise models that represent the submerse topography of rivers and reservoirs is desirable in order to construct an adequate database for analyzing geomorphologic changes, calculating water storage capacity, and making hydrologic simulations. These models can be generated by interpolating (x, y) bathymetry points. However, since extensive bathymetric surveys may prove to be costly and time consuming, measurements are usually made through cross-sectional surveys, which may lead to a sparse sampling pattern. Hybrid kriging methods, such as Regression Kriging (RK) and Co-Kriging (CK) employ the correlation with auxiliary predictors, as well as inter-variable correlation, to improve the predictions of the target variable. In this study, we introduced the orthogonal distance of a (x, y) point to the river centerline as an auxiliary variable for RK and CK. Given that river bed elevation variability is abrupt transversely to the flow direction, it is expected that the greater the Euclidean distance of a point to the thalweg, the greater the bed elevation will be. Hence, the aim of this study was to evaluate if the use of the orthogonal distance to centerline as an auxiliary variable for hybrid kriging methods improves the spatial prediction of river bed topography, when bathymetry data available is sparse. In order to asses such premise, we proposed two forms of external validation: in the first scenario, transversal cross-sections were used to make the spatial predictions, and the point data surveyed between sections was used as a testing dataset; in the second scenario, we randomly excluded 85% of the surveyed points from the training dataset, which were later used for testing the models. We compared the results from CK and RK to the ones obtained from Ordinary Kriging (OK), Inverse Distance Weighting (IDW) and Topogrid (TG). The bathymetric data for the study was surveyed in a 1.98 km flooded segment of the Grande River, located at the Funil hydroelectric power plant reservoir, in Minas Gerais, Brazil. Both external validation scenarios indicated that the employed RK method yielded the lowest RMSE among the analyzed interpolators. Moreover, the RK predictions were able to represent the thalweg between the widely spaced cross-sections, whereas the other methods under-predicted the river thalweg in such gaps. Therefore, we concluded that the employed RK method provided a simple approach for enhancing the quality of the spatial prediction from sparse bathymetry data.

Key-words: Geostatistics. River models. Spatial prediction.

RESUMO

A criação de modelos que representem a topografia submersa de rios e reservatórios de maneira contínua é desejável para se construir uma base de dados adequada para análise de mudanças geomorfológicas, cálculo de capacidade de armazenamento de água e para realização de simulações hidrológicas. Tais modelos são gerados pela interpolação de pontos (x,y) discretos de batimetria. Porém, considerando-se que levantamentos batimétricos extensivos despendem grande tempo e recursos, tais medições são geralmente realizadas através de seções batimétricas, que podem levar a formação de um padrão amostral esparso, devido às lacunas formadas entre as seções. Métodos híbridos de krigagem, como a krigagem por regressão (KR) e co-krigagem (CK), empregam a correlação com preditores auxiliares, além da auto-correlação entre variáveis, para melhorar a predição espacial da variável resposta. Neste estudo, sugeriu-se que a distância ortogonal de um ponto batimétrico (x,y) até a linha de centro do talvegue de um rio poderia ser usada como uma variável auxiliar para KR e CK. Considerando-se que a variabilidade espacial da cota do leito do rio é abrupta transversalmente a direção do fluxo, espera-se que quanto maior a distância euclidiana de um ponto até o talvegue, maior será sua elevação. Dessa forma, o objetivo desse estudo foi avaliar se o uso da distância ortogonal à linha de centro como variável auxiliar para métodos híbridos de krigagem pode melhorar a predição espacial da topografia do leito de rios e reservatórios, em casos de levantamentos batimétricos esparsos. Para analisar tal premissa, duas formas de validação externa foram propostas: na primeira, seções batimétricas transversais ao fluxo foram usadas para realizar as predições espaciais, enquanto os dados levantados entre tais seções foram usados como amostra de teste; na segunda, 85% dos pontos foram excluídos aleatoriamente da amostra de treino e, posteriormente, foram usados para validar as predições dos modelos. Os resultados da KR e da CK foram comparados aos obtidos por krigagem ordinária (KO), distância inversa ponderada (DIP) e Topogrid (TG). Os dados batimétricos utilizados neste estudo foram obtidos em um levantamento realizado em um trecho inundado do Rio Grande, com 1,98 km de comprimento, localizado no reservatório da usina hidrelétrica do Funil, no Sul do estado de Minas Gerais. Ambas as formas de validação indicaram que o método de KR aplicado resultou em menores valores de erro quadrático médio em relação aos demais interpoladores testados. Ademais, no mapa resultante da KR, o talvegue foi preservado nas grandes lacunas não amostradas entre as seções batimétricas, enquanto os demais métodos subestimaram a profundidade do talvegue em tais espaços. Assim, conclui-se que o método de KR empregado neste estudo propiciou uma abordagem simples para diminuir o erro da predição espacial a partir de dados esparsos de batimetria.

Palavras-chave: Geoestatística. Modelos fluviais. Predição espacial.

INTRODUCTION

River terrain models, which represent the submerse fluvial topography in a continuous manner, are useful for hydrologic simulations, as well as for the assessment of sediment transport and geomorphologic changes (GLENN et al., 2015; MERWADE, 2009). Such models are usually generated by interpolating discrete point data, obtained from bathymetric or topographic surveys (LEGLEITER, KYRIAKIDIS, 2008). Although LiDAR technology and multi-beam-echo-sounder sonar systems can provide high-resolution bathymetry data, single-beam-echo-sounders (SBES) offer a cost effective alternative for water depth measurements (JHA; MARIETHOZ; KELLY, 2013). Nevertheless, extensive sampling is still costly and time consuming. Therefore, river bathymetry is traditionally surveyed through cross-sections, which can be quickly recorded, using SBES sonar systems (SCHÄPPI et al., 2010; GLENN et al., 2015).

However, cross-sectional sampling patterns may not lead to precise river terrain models. One of the difficulties is that cross-sections can be isolated and widely spaced, which increases the gaps of unsampled areas, and reduces the quality of the spatial prediction (LEGLEITER, 2013). River morphology is another complicator regarding the interpolation of bathymetry data. According to Merwade, Maidment and Goff (2006), river bed topography is anisotropic: the channel elevation variability is greater transversely to the flow direction than it is along the flow direction; also, such anisotropy is not spatially consistent, given the river sinuosity.

In order to overcome these issues, some researchers have suggested that the spatial trend in river channels could be modeled by converting the Cartesian (x,y) coordinate system into a channel-centered (s, n) spatial referenced system, where the s-axis is oriented along the flow direction and the n-axis is

perpendicular to the flow (GOFF; NORDFJORD, 2004; MERWADE; MAIDMENT, HODGES, 2005; LEGLEITER; KYRIAKIDIS, 2008). Once this transformation is done, several functions, such as polynomial regression, splines and probability density function, can be used to remove the trend (MERWADE, 2009).

Although sofisticated geostatisical techniques have been developed for interpolating bathymetric data (LEGLEITER; KYRIAKIDIS, 2008; MERWADE; COOK; COONROD, 2008; MERWADE, 2009), few studies in Brazil have been dedicated to such theme (ALCÂNTRA et al., 2010; LOPES et al., 2013). Moreover, the interpolation of reservoir bathymetry data, which is used to calculate water storage capacity, has been usually applied through mechanical spatial prediction methods (e. g. ALBERTIN et al., 2010; MIRANDA et al., 2013). Such methods, although simple and flexible, can be considered subjective and empirical, and provide no intrinsic estimation of the model error (HENGL, 2009). The discrepancy between the availability of spatial prediction techniques for discrete bathymetry data and their use in Brazilian research may lie in the scarcity of available data, which renders the more sophisticated models non-applicable. Also, coordinate transformation is not a common automatic feature for Geographic Information Systems (GIS), thus requiring some programming efforts that may not always be feasible.

In geostatistics, kriging techniques are considered to offer the best unbiased linear predictions (BLUP). That is, the linear equations from the kriging system provide estimations with a mean residual error equal to 0 and with minimum variance (ISAAKS; SRIVASTAVA, 1989; OLIVER; WEBSTER, 2014). Hybrid kriging methods, such as co-kriging and regression kriging, employ not only the spatial auto-correlation of the target variable, but also the inter-variable correlation, and the correlation with auxiliary predictors

(ODEH; MCBRATNEY; CHITTLEBOROUGH, 2006; HENGL, 2009). Therefore, auxiliary maps with spatially exhaustive information are used to improve the predictions based on point observations of the target variable (HENGL; HEUVELINK; ROSSITER, 2007). Hybrid kriging methods have been widely used in several environmental sciences, such as topographic modeling (HENGL et al., 2008), soil science (ODEH; MCBRATNEY; CHITTLEBOROUGH, 2006; ZHU; LIN; 2010; WATT; PALMER, 2012; QI-YONG et al., 2014), meteorology (JOYNER et al., 2015) and marine sedimentology (JEROSCH, 2013).

In this study, we hypothesized that, when dealing with sparse river bathymetry data, the orthogonal distance to the river centerline could be used as an auxiliary variable for hybrid kriging methods. Instead of converting the Cartesian coordinate system into a channel oriented system, we used the proposed auxiliary variable as a proxy for modeling the spatial trend of river bed topography. The auxiliary variable was employed for regression kriging (RK) and co-kriging (CK). We compared the performance of these techniques with the results from ordinary kriging (OK) and straight forward mechanical interpolators: Inverse Distance Weighting (IDW) and Topogrid (TG).

MATERIAL AND METHODS

Study area and bathymetric survey

This study is based on a bathymetric survey from a flooded segment of the Grande River, located in the Funil hydroelectric power plant reservoir, between the municipalities of Lavras and Perdões, in the southern region of the state of Minas Gerais, Brazil (Figure 1). The survey was conducted in January 2015 as part of a reevaluation study of the water storage capacity of the Funil reservoir.

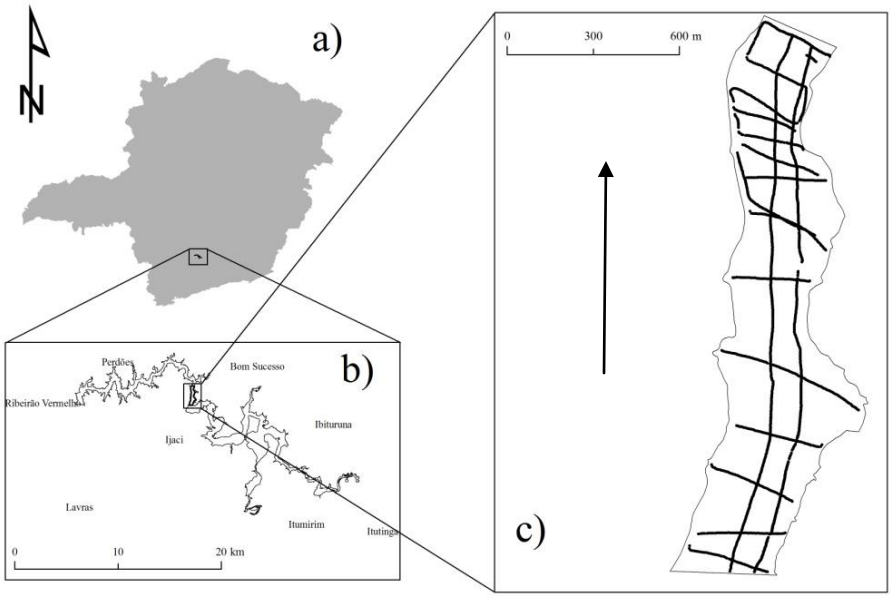

Figure 1 Location of the study area: a) State of Minas Gerais, Brazil; b) Reservoir of the Funil hydroelectric power plant; c) Studied segment of the Grande River: lines indicate the surveyed cross-sections, and arrow indicates flow direction

A SBES attached to a motorized boat was used to measure water depth at (x,y) point locations. The survey was executed through cross-sections, transversely and longitudinally to the river flow direction (Figure 1). For each cross-section, water level was measured using Real Time Kinetics Global Positional System (RTK GPS) technology. The base of the device was fixated on a georeferenced mark, and the rover connected to the boat. The river bed elevation values (z) for each (x,y) point were calculated by subtracting water level from water depth. The survey covered a total of 2,326 point locations.

The segment of the Grande River is 1.98 km in length, and has an average width of 323 m. Although the area is located in a reservoir, the segment still preserves river morphology. The motivation for this study came precisely

from the fact that, when interpolating the Funil reservoir bathymetry data, we came to notice that most of the flooded area still maintained river morphology, which brings us back to all the obstacles previously discussed, regarding river bed spatial modeling.

Auxiliary variable

The spatial variability of river bed topography is abrupt transversally to the water flow direction (Figure 2). Due to such morphologic characteristic, it is expected that the greater the orthogonal distance of a (x,y) point to the river thalweg centerline, the greater the river bed elevation (z) will be.

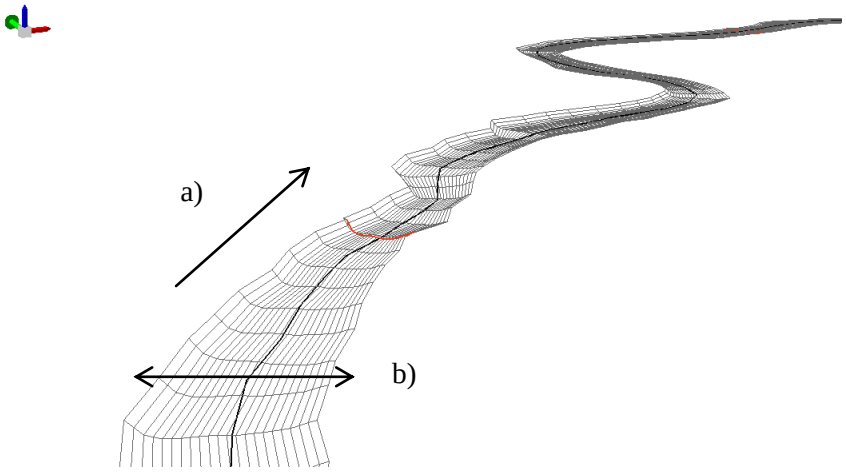

Figure 2 3D mesh of a river channel: bed elevation variability is smoother along flow direction (a), than across flow direction (b)

The river thalweg, i.e. a centerline along the lowest elevations of the water flow direction, was identified by using a simplified adaptation of the methodology suggested by Merwade, Maidment and Hodges (2005). Firstly, a mechanical method with low computational demand was used to interpolate the observed point data. Secondly, the sampled point data was divided in quantiles, according to the elevation values (z). The symbology of the points was then

altered depending on the quantiles, allowing the visual identification of the lowest elevation values within the cross-sections. Finally, the thalweg centerline was manually drawn, using editing tools, following the lowest values from the interpolated surface and the point symbology.

The orthogonal distance to the centerline was obtained using the Euclidean Distance tool, from ArcMap 10.1 (ESRI, 2011), which generates a grid raster where the cell values represent the minimum distance of a given location to a given vector (in this case, the centerline) (Figure 3). Since the grid cell resolution of such raster is arbitrary, we evaluated the results from 1, 3, 5, 10 and 15 m. The grid cell values generated by the Euclidean Distance tool were extracted at the sampled locations of the target variable. A linear model was then adjusted for bed elevation (Y) in function of the orthogonal distance to the centerline (X).

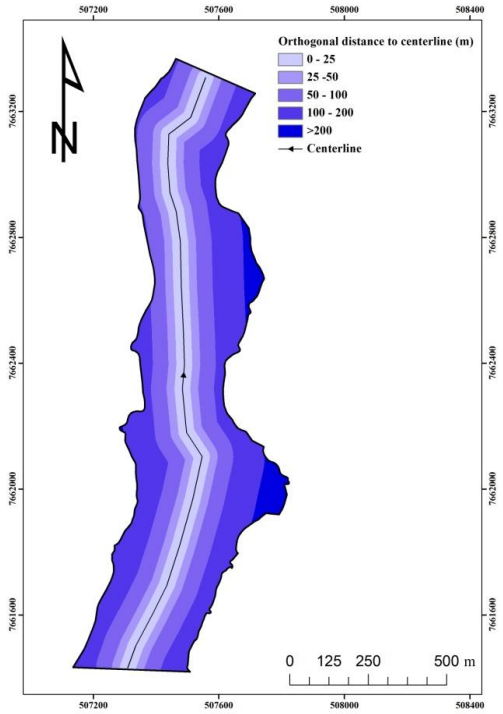

Figure 3 Raster of the orthogonal distance to river centerline

Data analysis

Summary statistics from the bathymetric survey was calculated in R package GeoR (RIBEIRO JR.; DIGGLE, 2001).

The spatial trend of the dataset was evaluated both in GeoR (RIBEIRO JR.; DIGGLE, 2001), and in the geostatistical analyst toolset of ArcGIS 10.1 (ESRI, 2011). A polynomial regression on coordinates was performed in order to model the data trend for the OK and CK methods.

For the kriging methods, the semivariograms were modeled after plotting the semivariances (γ) between the sampled values of the target variable (HENGL, 2009):

$$\gamma(h) = \frac{1}{2} E[(z(s_i) - z(s_i + h))^2] \quad (1)$$

where: $z(s_i)$ is the value of the target variable at a given location and $z(s_i + h)$ is the value of the variable at a distance h.

For CK, the cross variogram cloud was plotted according to equation 2 (Webster; Oliver, 2007):

$$\gamma(h) = \frac{1}{2} E[(z(s_i) - z(s_i + h)) * (y(s_i) - y(s_i + h))] \quad (2)$$

where: $z(s_i)$ is the value of the target variable at an s_i location; $z(s_i + h)$ is the value of the variable at a distance h; $y(s_i)$ is the value of the co-variable at an s_i location, and $y(s_i + h)$ is the value of the co-variable at a distance h.

Geostatistical spatial prediction methods

In OK, the spatial prediction of a target variable (z) at an unsampled location (s_0) is calculated as:

$$z^*(s_o) = \sum_{i=1}^{n} \lambda_i z(s_i) \quad (3)$$

where: n is the number of s_i observations of the target variable, and λ_i are the kriging weights chosen to minimize error variance (σ^2) between sampled (s_i) and estimated values (s_0) (OLIVER; WEBSTER, 2014):

$$\sigma^2 = \sum_{i=1}^{n} \lambda_i + \gamma(s_i, s_0) + \varphi \tag{4}$$

$$\sum_{i=1}^{n} \lambda_i = 1 \tag{5}$$

where: φ is the Lagrange multiplier, which optimizes kriging variance (ODEH; MCBRATNEY; CHITTLEBOROUGH, 2006)

CK estimations are based the spatial auto-correlation of the target variable and the auxiliary variables (ISAAKS; SRIVASTAVA, 1989):

$$z^*(s_o) = \sum_{i=1}^{n} a_i z(s_i) + \sum_{j=1}^{m} b_j w(s_j) \tag{6}$$

where: n is the number of s_i observations of the target variable z; m is the number of s_j observations of the auxiliary variable w, and a_i and b_j are the co-kriging weights.

RK predicts the values of a target variable z at an unsampled location s_0 as the sum of the deterministic component of the signal process estimated by a fitted linear model plus the residual of such model, which is interpolated using ordinary kriging (HENGL; HEUVELINK; ROSSITER, 2007; HENGL; HEUVELINK; STEIN, 2004):

$$\hat{z}(s_o) = \hat{\beta}(s_o) * q(s_0) + \sum_{i=1}^{n} \lambda_i (s_0) * e(s_i) \quad (5)$$

where: $\hat{\beta}(s_o)$ are the regression coefficients from the deterministic component; $q(s_o)$ is the auxiliary variable at s_o; $w_i(s_o)$ are the kriging weights, and $e(s_i)$ are the regression residuals.

In this study, the computational steps for the RK method can be summarized as:

1. Once the linear model of the target variable in function of the auxiliary variable was fitted, the adjusted equation was applied to the auxiliary grid raster, using map algebra tools;
2. The regression residuals were calculated by subtracting the observed values of the target variable from the ones estimated by the model;
3. The residuals from the model were interpolated by OK;
4. The regression model grid raster was added to the interpolated residual surface using map algebra tools.

Mechanical spatial prediction methods

IDW estimates the value of the target variable at an unsampled location by using the same equation as the OK method does (Equation 3). However, in IDW the weights (λ_i) depend only on the distance from sampled points:

$$\lambda_i = \frac{\frac{1}{d_i^P}}{\sum_{i=1}^{n} \frac{1}{d_i^P}} \quad (3)$$

where: d_i is the distance between the unsampled location (s_0) and the *i*th sampled location (s_i) , and *P* is the power variable, most commonly set to two (MERWADE; MAIDMENT; GOFF, 2006).

Topogrid (TG) is an interpolation method designed for creating hydrologically correct Digital Elevation Models (DEM). The method is based on a morphological approach, which removes spurious pits and enforces the drainage network. The algorithms for the method are thoroughly displayed in Hutchinson (1989). In this study, we used the Topo to Raster tool, from ArcGIS 10.1 (ESRI, 2011), which automates the TG procedure.

Validation

In order to evaluate the spatial prediction methods in a situation of sparse bathymetry data, we proposed two forms of external validation. In the first scenario, we analyzed the efficiency of the interpolators under a traditional bathymetric survey. The transversal cross-section data was used as the training dataset, which consisted of approximately 40% the total 2,326 available point samples. The average spacing between cross-sections was of 166 m. The data surveyed between such cross-sections was used as the testing dataset (Figure 4a). In the second validation scenario, we randomly excluded 85% of the available point data, in order to simulate a very restricted sampling pattern. The remaining 15% of the sampled data was used as the training dataset. The excluded points were later used as testing data (Figure 4b).

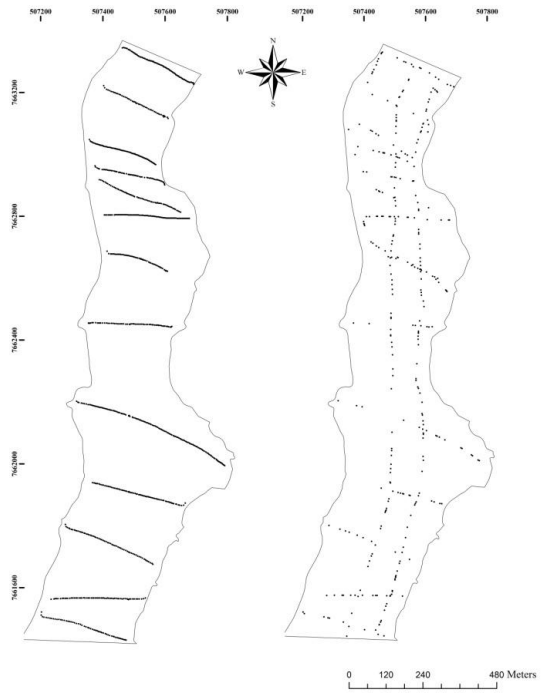

Figure 4 Training datasets: Cross-sectional sampling pattern (a), and random exclusion of sampled points (b)

Model accuracy was evaluated according to the residual Mean Error (ME), and Root Mean Squared Error (RMSE):

$$EM = \frac{1}{n}\sum_{i=1}^{n}(Z - Z^{*}) \tag{6}$$

$$REQM = \sqrt{\frac{1}{n}\sum_{i=1}^{n}[(Z - Z^{*})]^{2}} \tag{7}$$

where: Z is the observed value of the target variable in a (x,y) point; Z^* is the predicted value in such point, and n is the number of samples from the testing dataset.

Regression analysis of the predicted and observed values was also evaluated.

RESULTS AND DISCUSSION

The descriptive statistics of the two training datasets are displayed in Table 1.

Table 1 Descriptive statistics of the training datasets

Parameter	CS	RA
	Value (m)	
Minimum	779.5	782.7
Maximum	807.2	807.2
Mean	795.3	795.1
Median	794.0	793.0
Standard deviation	4.96	4.86

Legend: CS: Cross-section sampling pattern; RA: Random exclusion of sampled points

The orthogonal distance to river centerline presented a significant positive correlation with river bed elevation on all the evaluated grid cell resolutions ($p < 0.05$). Hence, we used the 1 m resolution map. Due to the strong

correlation between the auxiliary variable and the target variable, most of the spatial variability of river bed topography could be deterministically modeled (Figure 5). For the cross-sectional dataset, 53% of the spatial prediction was modeled according to a linear regression of elevation as a function of the orthogonal distance to river centerline. For the random exclusion training dataset, the regression from the auxiliary variable accounted for 60% of the river bed spatial variability.

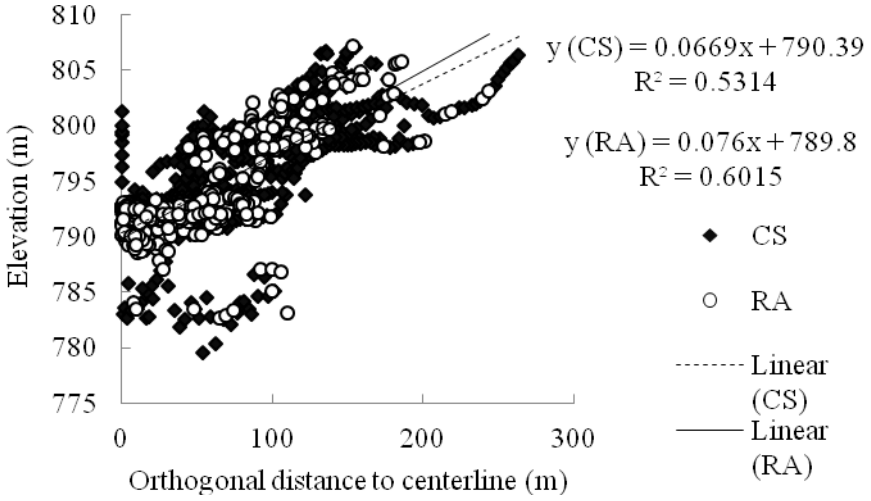

Figure 5. Linear models of the target variable in function of the auxiliary variable, for the two testing datasets. Legend: CS: Cross-sectional sampling pattern; RA: Random exclusion of sampling points

In the segment of the Grande River that was studied, flow direction is roughly oriented from South to North (Figure 1). Hence, trend analysis showed a decrease in channel elevation with the increase of the Y coordinate, due to river bed slope (Figure 6b, Figure 9b). Such trend had an overall smooth behavior, except in the northern portion of the segment, where elevation decreases more abruptly. The trend in the direction of the X coordinate is much more evident.

Figures 6a and 9a demonstrate how river bed elevation, clearly influenced by the river thalweg, is lower in the central region of the scatter plot.

The polynomial regression on coordinates, which was used to model the trend for the OK and CK methods, yielded residuals with a trend behavior displayed in Figures 7 and 10. Trend analyses of the residuals from the regression as a function of the auxiliary variable are displayed in Figures 8 and 11.

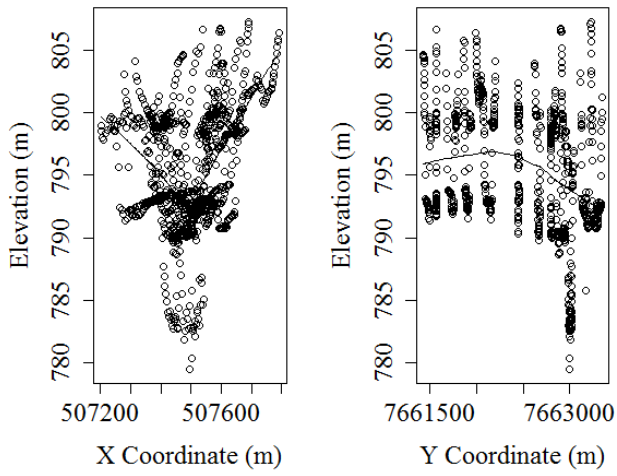

Figure 6 Trend of the target variable, for the cross-sectional training dataset

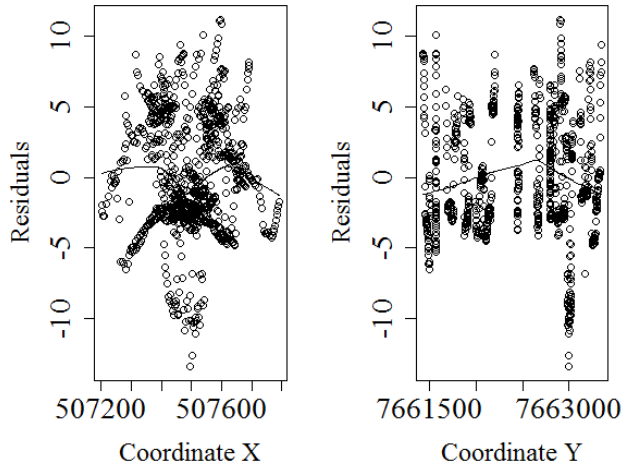

Figure 7 Trend of residuals from the cubic polynomial regression of the target variable in function of the (x,y) coordinates, for the cross-sectional training dataset

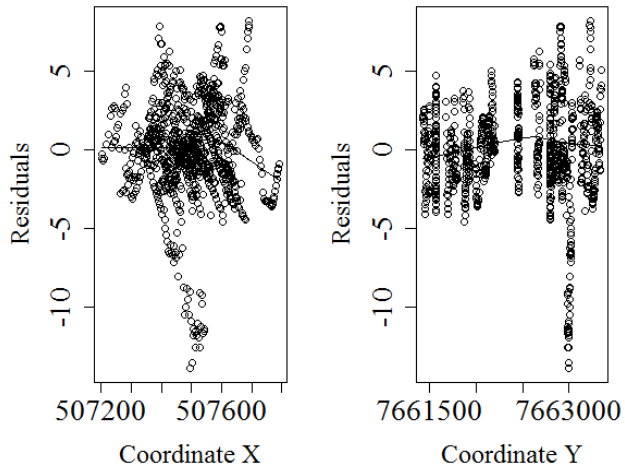

Figure 8 Trend of residuals from the regression of the target variable in function of the auxiliary variable, for the cross-sectional training dataset

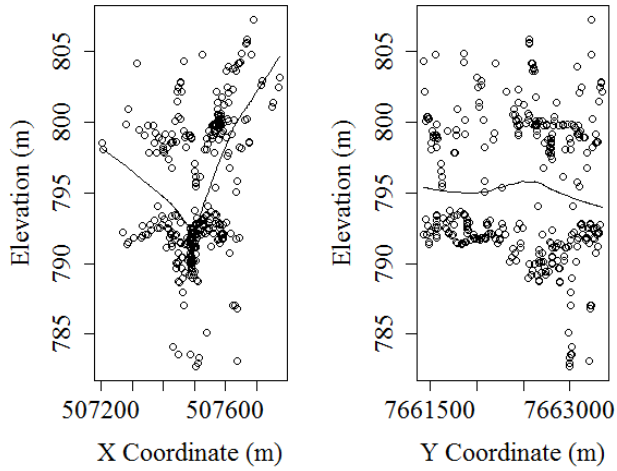

Figure 9 Trend of the target variable, for the random exclusion of sampling points training dataset

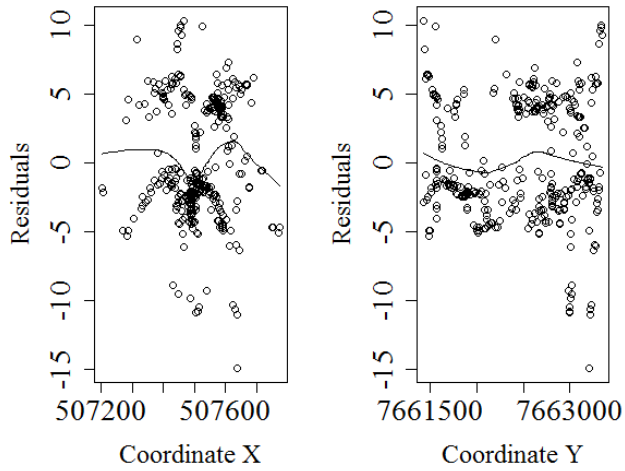

Figure 10 Trend of residuals from the cubic polynomial regression of the target variable in function of the (x,y) coordinates, for the random exclusion training dataset

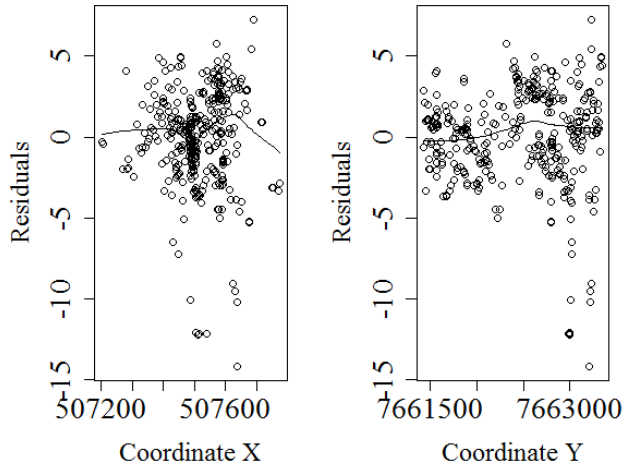

Figure 11 Trend of residuals from the regression of the target variable in function of the auxiliary variable, for the random exclusion training dataset

The trend lines from Figures 8 and 11 demonstrate how the regression from the auxiliary variable modeled the spatial trend more adequately than the regression on coordinates. Although the residuals from the latter method smoothed the trend in comparison to the data, the residuals from first method displayed straighter trend lines. Moreover, one could hypothesize that regression on coordinates was only able to model the spatial trend due to the low sinuosity and orientation of the flow direction of the river segment; whereas the regression from the auxiliary variable would not be limited by such morphologic characteristics. However, different datasets would be necessary to confirm such hypothesis.

Figures 12 and 13 display the experimental and modeled variograms for each of the employed spatial prediction techniques. For the cross-sectional training dataset, the semivariogram of the regression residuals was fitted into a stable model (C_0=0.71; C_1=14.59; R=108.32) (Figure 12). The sill and the range

values of the model were respectively 22% and 23% lower than the ones observed for the target variable semivariogram, which was fitted into a spherical model (C_0=0.02; C_1=18.63; R=135.68). Such behavior indicates that the feature-space structure has decreased due to the effective removal of the external drift (HENGL; HEUVELINK; STEIN, 2004; HENGL; HEUVELINK; ROSSITER, 2007). The cross-variogram was also fitted into a spherical model, with similar parameters as the variogram of the target variable (C_0=0.01; C_1=20.00; R=139.98). The variograms from the random exclusion training dataset (Figure 13) displayed an analogous pattern. The residual semivariogram (spherical; C_0=0.03; C_1=9.05; R=77.75) presented sill and range values that were about 40% lower than the ones from the target variable semivariogram (spherical; C_0=0.00; C_1=14.98; R=130.71), and from the cross-variogram (spherical; C_0=0.00; C_1=15.34; R=140.00).

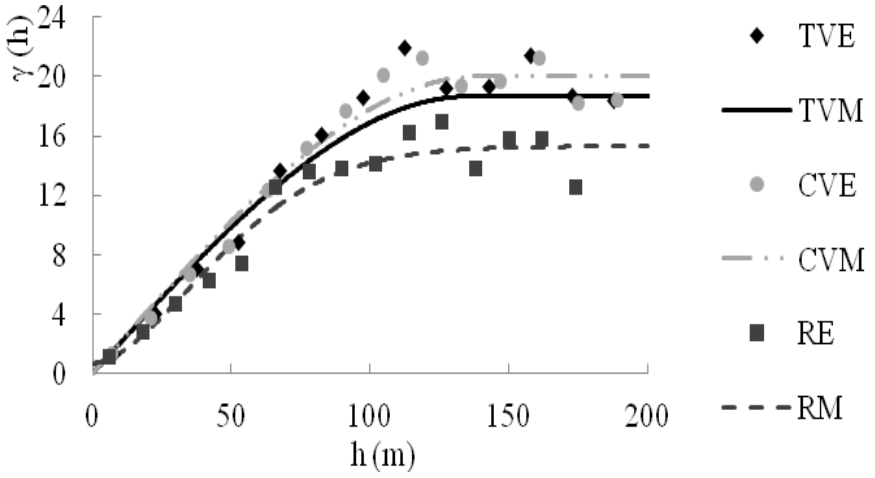

Figure 12. Semivariograms of the cross-sectional training dataset for the kriging method Legend: TVE: experimental semivariogram of the target variable; TVM: Modeled semivariogram of the target variable; CVE: experimental cross-variogram; CVM: modeled cross-variogram; RE: experimental semivariogram of the residuals; RM: modeled semivariogram of the residuals

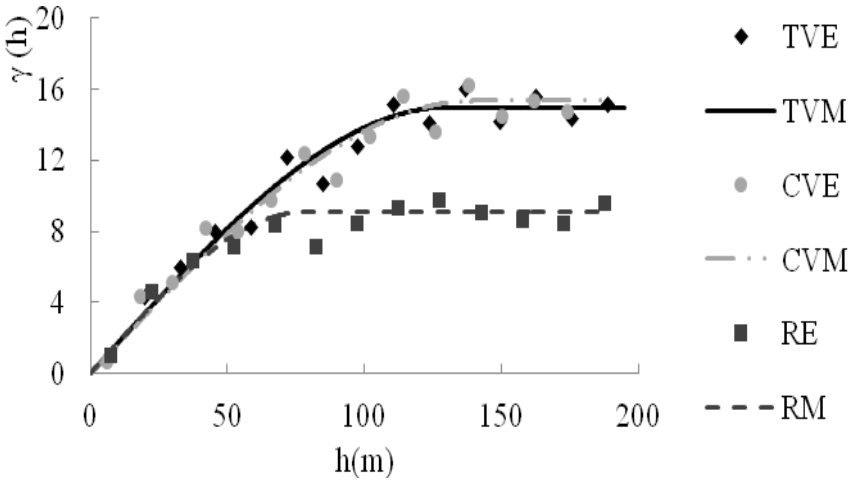

Figure 13 Semivariograms of the random exclusion training dataset for each kriging method. Legend: TVE: experimental semivariogram of the target variable; TVM: Modeled semivariogram of the target variable; CVE: experimental cross-variogram; CVM: modeled cross-variogram; RE: experimental semivariogram of the residuals; RM: modeled semivariogram of the residuals.

The external validation exhibited a better performance of the geostatistical methods for the cross-sectional dataset (Table 2). The ME for such methods, in comparison to the mechanical interpolators, was much closer to zero, given the unbiased character of the kriging equations. The RMSE was lower for RK, with a relative decrease of 11% over OK and CK. The regression between the observed and estimated values yielded a higher R^2 for RK, with a relative increment of 15% over OK and CK. The ME values for IDW and TG demonstrated a clear bias in the spatial predictions, which severely under-estimated the river bed elevation in the gaps between the cross-sections. The RMSE values for IDW and TG were almost twice higher than those for RK.

Table 2 Results from the cross-sectional dataset validation

Method	CS

	ME	RMSE	R^2
OK	-0.09	2.97	58.11
CK	-0.09	2.96	58.38
RK	-0.12	2.64	67.16
IDW	-2.58	5.02	53.91
TG	-3.12	4.85	44.79

Legend: OK: Ordinary Kriging; CK: Co-Kriging; RK: Regression Kriging; IDW: Inverse Distance Weighting; TG: Topogrid. RMSE: Root mean squared error.

In the RK map (Figure 14e) the greater depth along the river thalweg was preserved between the cross-sections. Such behavior was not observed in the OK, CK, IDW and TG maps, although the same auxiliary variable was used in CK. According to Hengl, Heuvelink and Rossiter (2007), CK is not developed for situations where the spatial information of the auxiliary variable is exhaustive, i.e. when the covariates are available as maps..Such characteristic may explain the worst performance of CK compared to RK in this study. Moreover, we can hypothesize that the lack of inter-variable spatial cross-correlation hampered a better performance from the CK method.

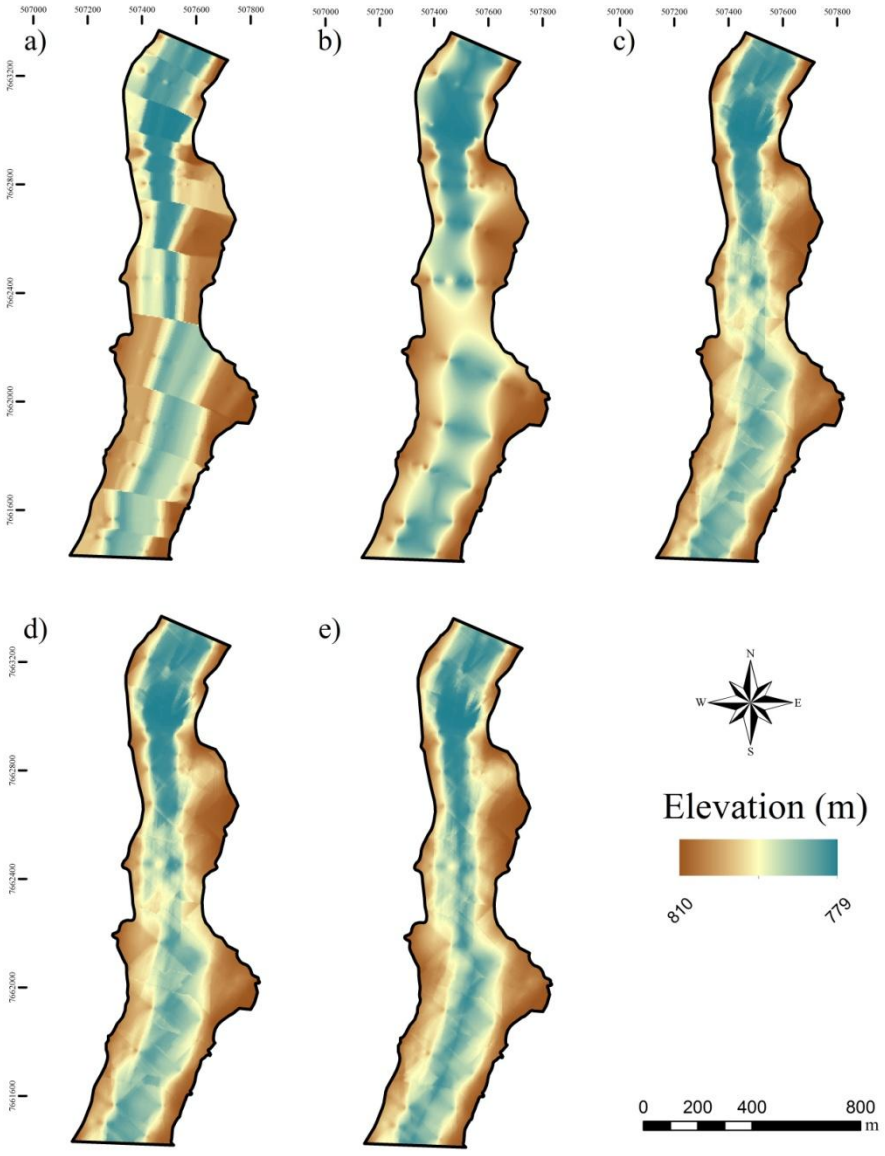

Figure 14 Spatial prediction maps of bed elevation in the studied segment of the Grande River, cross-sectional training dataset: a) Inverse Distance Weighting; b) Topogrid; c) Ordinary Kriging; d) Co-Kriging; e) Regression Kriging

Due to the significant non-spatial correlation between the auxiliary variable and the target variable, the RK map shows the influence of the orthogonal distance to the river centerline, which contributed to a more adequate representation the river thalweg in the unsurveyed areas. The results from RK in the external validation indicate that the method yielded more accurate predictions between the cross-sections, possibly because the other interpolators under-predicted the river thalweg in the unsampled gaps. As displayed in Figure 14, the OK, CK, IDW and TG maps presented discontinuous "hot-spots" of lower elevation where the cross-sections were located. According to Legleiter and Kyriakidis (2008), OK predictions are not accurate when cross-sections are sparse, leading to an under-prediction of the river thalweg. The authors also state that in such scenario of coarse available data, kriging with an external drift offers more precise predictions. According to the authors, the estimations rely heavily on the underlying deterministic model: since the spatial auto-correlation of the target variable drastically decreases where the point observations become farther apart from each other, the spatial variability of the target variable is almost entirely modeled by the auxiliary variable, or the external drift.

In the random exclusion dataset, the validation demonstrated a more similar performance among the spatial prediction methods (Table 3). Although the kriging methods still yielded ME values closer to zero when compared to the mechanical interpolators, the difference was not as pronounced as in the cross-sectional dataset. RK provided the lowest RMSE, which decreased 7% in relation to OK, the second best predictor according to the validation. In order to verify if RK would still yield better estimations based on a less restricted database, we simulated two other scenarios, in which we randomly excluded 70% and 50% of the sampled points. In such situations, however, the external validation demonstrated no improvement from the RK results in comparison to OK.

Table 3 Results from the random exclusion dataset validation

Method	CS		
	ME	RMSE	R^2
OK	0.19	1.42	90.86
CK	0.18	1.43	90.77
RK	0.18	1.32	92.13
IDW	0.38	1.86	84.72
TG	0.25	1.47	90.53

Legend: OK: Ordinary Kriging; CK: Co-Kriging; RK: Regression Kriging; IDW: Inverse Distance Weighting; TG: Topogrid. RMSE: Root mean squared error.

The results from the validation of the random exclusion dataset demonstrated that in all spatial prediction methods the RMSE decreased considerably in relation to the cross-sectional dataset. Even though in the random exclusion dataset the number of observed points was about three times lower than in the cross-sectional dataset, the sampling pattern, in the first case, produced fewer gaps of unsampled areas. Hence, predictions were mostly based on point observations that were closer to each other. Also, in the cross-sectional dataset, the testing points were very distant from the training points, which increases the rigorosity of the validation.

Figure 15 displays the spatial prediction maps from the random exclusion dataset. Here, the resulting maps from the different interpolators had more in common than the ones from the cross-sectional dataset.

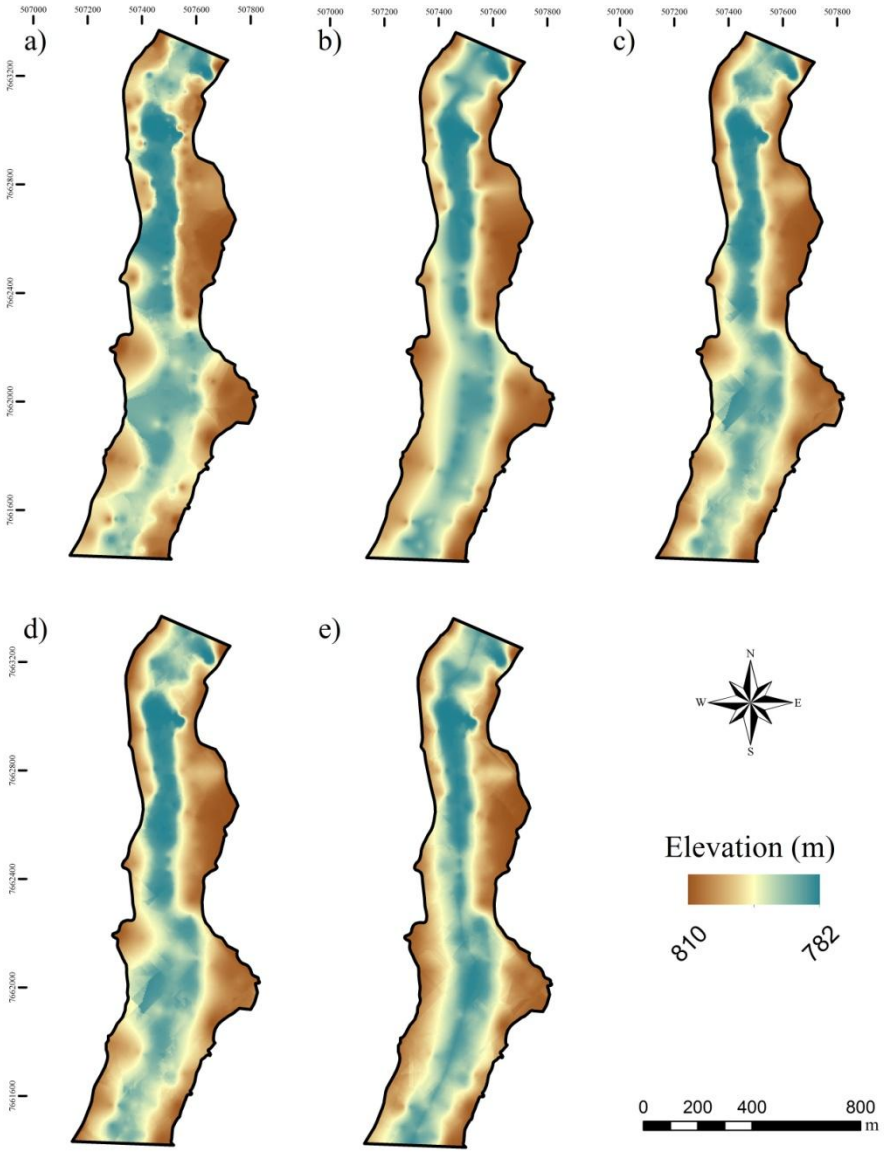

Figure 15 Spatial prediction maps of bed elevation in the segment of the Grande River studied, random exclusion training dataset: a) Inverse Distance Weighting; b) Topogrid; c) Ordinary Kriging; d) Co-Kriging; e) Regression Kriging

The OK and CK maps (Figure 15c, d) were able to represent the thalweg more adequately than when the cross-sectional dataset was used. In the RK map (Figure 15e), the influence of the auxiliary variable is still clear, since the transition from the original river channel to the floodplain seems smoother. Also, "hot-spots" from the observed data are not as pronounced as in the other spatial prediction maps.

The standard error maps from the employed kriging methods also demonstrate that greater uncertainty was associated to the cross-sectional dataset estimations (Figure 16). As the distance between sections increases, so does the standard error values in the large unsurveyed gaps. Although a smaller number of point data was used to interpolate the random exclusion training dataset, the standard error maps show that the sampling pattern provided means for more accurate estimations (Figure 17).

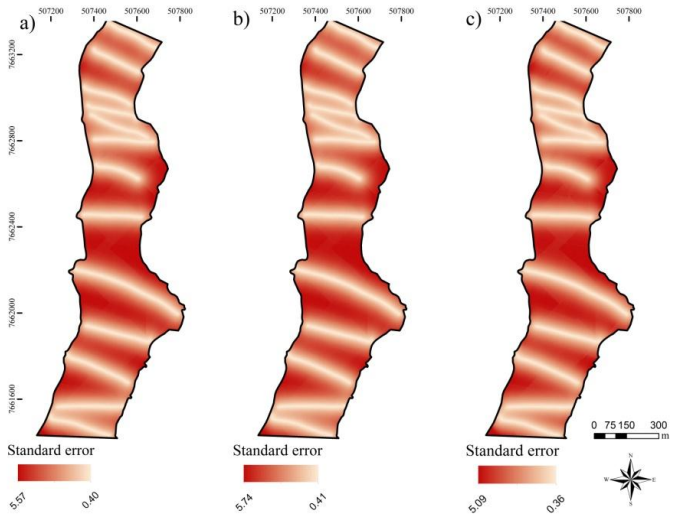

Figure 16. Standard error maps of in the segment of the Grande River studied, cross-sectional training dataset: a) Ordinary Kriging; b) Co-Kriging; c) Ordinary Kriging of residuals.

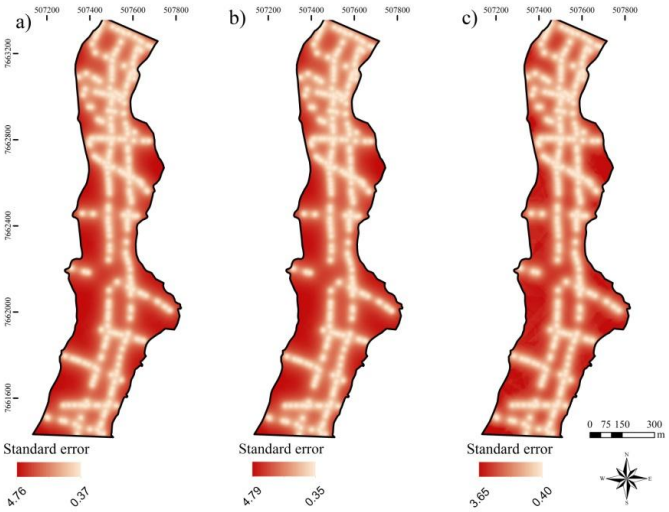

Figure 17. Standard error maps of in the studied segment of the Grande River, random exclusion training dataset: a) Ordinary Kriging; b) Co-Kriging; c) Ordinary Kriging of residuals.

CONCLUSIONS

The use of the orthogonal distance to river centerline as an auxiliary variable for hybrid kriging methods improved the estimations of river bed topography, but only in the RK predictions. In such case, the regression on the auxiliary variable was able to model the spatial trend of the target variable more adequately than the regression on coordinates. In both validation scenarios of sparse bathymetry data, the proposed auxiliary variable enhanced the spatial prediction of the target variable Also, especially in the cross-sectional dataset, RK was able to represent the continuity of the river thalweg in the wide unsurveyed gaps. Hence, the modeling of the deterministic component of the spatial variability of river bed elevation based on the orthogonal distance of a point to the river centerline can be an effective and simple approach to improve the interpolation of sparse bathymetry data.

REFERENCES

ALBERTIN, L. L.; MATOS, A. J. S.; MAUAD, F. F. Cálculo do Volume e Análise da Deposição de Sedimentos do Reservatório de Três Irmãos. **Revista Brasileira de Recursos Hídricos**, v. 15, p.57-67, 2010.

ALCÂNTRA, E.; NOVO, E.; STECH, J.; ASSIREU, A.; NASCIMENTO, R.; LORENZZETTI, J.; SOUZA, A. Integrating historical topographic maps and SRTM data to derive the bathymetry of a tropical reservoir. **Journal of Hydrology**, v.389, p.311-316, 2010.

ENVIRONMENTAL SYSTEMS RESEARCH INSTITUTE – ESRI. ArcGIS for Desktop, version 10.1. Redlands, 2011. CD ROM.

GLENN, J; TONINA, D.; MOREHEAD, M. D.; FIEDLER, F.; BENJAKAR, R. Effect of transect location, transect spacing and interpolation methods on river bathymetry accuracy. **Earth Surface Processes and Landforms**, p. n/a–n/a, 2015.

GOFF, J. A.; NORDFJORD, S. Interpolation of fluvial morphology using channel-oriented coordinate transformation: A case study from the New Jersey Shelf. **Mathematical Geology**, v. 36, n.6, p.643–658, 2004.

HENGL, T.; HEUVELINK, G. B. M.; STEIN, A. A generic framework for spatial prediction of soil variables based on regression-kriging. **Geoderna**, v.120, p. 75-93, 2004.

HENGL, T.; HEUVELINK, G. B. M.; ROSSITER, D. G. About regression-kriging: From equations to case studies. **Computers & Geosciences**, v. 33, p.1301-1315, 2007.

HENGL, T.; BAJAT, B.; BLAGOJEVIC, D.; REUTER, H. I.; Geostatistical modeling of topography using auxiliary maps. **Computers & Geosciences**, v.34, p. 1886-1899, 2008.

HENGL, T. **A Practical Guide to Geostatiscal Mapping**. Luxembourg: Office for Official Publications of the European Communities, 2009. 143 p.

HUTCHINSON, M. F. A new procedure for gridding elevation and stream line data with automatic removal of spurious pits. **Journal of Hydrology**, v. 106, p. 211–232, 1989.

ISAAKS, E. H.; SRIVASTAVA, R. M. **Applied Geostatistics.** New York: Oxford University Press, 1989. 547 p.

JEROSCH, K. Geostatistical mapping and spatial variability of surficial sediment types on the Beaufort Shelf based on grain size data. **Journal of Marine Systems**, v. 127, p.5-13, 2013.

JHA, S. K.; MARIETHOZ, G.; KELLY, B. F. J. Bathymetry fusion using multiple-point geostatistics: Novelty and challenges in representing non-stationary bedforms. **Environmental Modelling & Software**, v. 50, p. 66–76, 2013.

JOYNER, T. A.; FREIDLAND, C. J.; ROHLI, R. V.; TREVIÑO, A. M.; MASSARRA, C.; PAULUS, G. Cross-correlation modeling of European windstorms: A cokriging approach for optimizing surface wind estimates. **Spatial Statistics**, v. 13, p. 62–75, 2015.

LEGLEITER, C. J. Mapping river depth from publicly available aerial images. **River Research and Applications**, v. 29, p. 760–780, 2013.

LEGLEITER, C. J.; KYRIAKIDIS, P. C. Spatial prediction of river channel topography by kriging. **Earth Surface Processes and Landforms**, v. 33, p. 841–867, 2008.

LOPES, H. L.; NETO, A. R.; CIRILO, J. A. Modelagem batimétrica no reservatório de Sobradinho: I – geração e avaliação de superfícies batimétricas utilizando interpoladores espaciais. **Revista Brasileira de Cartografia**, v. 65, p.907-922, 2013.

MERWADE, V. M.; MAIDMENT, D. R.; HODGES, B. R. Geospatial Representation of River Channels. **Journal of Hydrologic Engineering,** v. 10, p. 243–251, 2005.

MERWADE, V. M.; MAIDMENT, D. R.; GOFF, J. A. Anisotropic considerations while interpolating river channel bathymetry. **Journal of Hydrology**, v. 331, n. 3-4, p. 731–741, 2006.

MERWADE, V.; COOK, A.; COONROD, J. GIS techniques for creating river terrain models for hydrodynamic modeling and flood inundation mapping. **Environmental Modelling & Software**, v.23, p.1300-1311, 2008.

MERWADE, V. Effect of spatial trends on interpolation of river bathymetry. **Journal of Hydrology**, v. 371, n. 1-4, p. 169–181, 2009.

MIRANDA, R. B.; SCARPINELA, G. A.; MAUAD, F. F. Influência do assoreamento na capacidade de armazenamento do Reservatório da usina hidrelétrica de Três Irmãos (SP/BRASIL). **Revista Recursos Hídricos**, v.34, p.69-79, 2013.

ODEH, I. O. A.; MCBRATNEY, A. B.; CHITTLEBOROUGH, D. J. Spatial prediction of soil properties from landform attributes derived from a digital elevation model. **Geoderma**, v. 63, p. 197–214, 2006.

OLIVER, M. A.; WEBSTER, R. A tutorial guide to geostatistics: Computing and modelling variograms and kriging. **Catena**, v. 113, p. 56–69, 2014.

QI-YONG, Y.; JIANG, Z. C.; LI, W. J.; HUI, L. Prediction of soil organic matter in peak-cluster depression region using kriging and terrain indices. **Soil and Tillage Research,** v. 144, p. 126–132, 2014.

RIBEIRO JR.; P. J.; DIGGLE, P. J. geoR: A package for geostatistical analysis. R-News, v.1, n.2, 2001.

SCHÄPPI, B.; PERONA, P.; SCHNEIDER, P.; BURLANDO, P. Integrating river cross section measurements with digital terrain models for improved flow modelling applications. **Computers & Geosciences**, v.36, p.707-716, 2010.

WATT, M. S.; PALMER, D. J. Use of regression kriging to develop a Carbon:Nitrogen ratio surface for New Zealand. **Geoderma**, v. 183-184, p. 49–57, 2012.

WEBSTER, R.; OLIVER, M. A. **Geostatistics for environmental scientists.** West Sussex: John Wiley & Sons, 2007. 315 p.

ZHU, Q.; LIN, H. S. Comparing Ordinary Kriging and Regression Kriging for Soil Properties in Contrasting Landscapes. **Pedosphere**, v. 20, n. 5, p. 594–606, 2010.